

## Noble Gas–Actinide Complexes of the CUO Molecule with Multiple Ar, Kr, and Xe Atoms in Noble-Gas Matrices

Lester Andrews\*<sup>†</sup>, Binyong Liang,<sup>†</sup> Jun Li,<sup>‡</sup> and Bruce E. Bursten\*<sup>§</sup>

Contribution from the Department of Chemistry, University of Virginia, Charlottesville, Virginia 22904-4319, William R. Wiley Environmental Molecular Sciences Laboratory, Pacific Northwest National Laboratory, Richland, Washington 99352, and the Department of Chemistry, The Ohio State University, Columbus, Ohio 43210

Received July 23, 2002; E-mail: isa@virginia.edu

**Abstract:** Laser-ablated U atoms react with CO in excess argon to produce CUO, which is trapped in a triplet state in solid argon at 7 K, based on agreement between observed and relativistic density functional theory (DFT) calculated isotopic frequencies (<sup>12</sup>C<sup>16</sup>O, <sup>13</sup>C<sup>16</sup>O, <sup>12</sup>C<sup>18</sup>O). This observation contrasts a recent neon matrix investigation, which trapped CUO in a linear singlet state calculated to be about 1 kcal/mol lower in energy. Experiments with krypton and xenon give results analogous to those with argon. Similar work with dilute Kr and Xe in argon finds small frequency shifts in new four-band progressions for CUO in the same triplet states trapped in solid argon and provides evidence for four distinct CUO(Ar)<sub>4-n</sub>(Ng)<sub>n</sub> (Ng = Kr, Xe, n = 1, 2, 3, 4) complexes for each Ng. DFT calculations show that successively higher Ng complexes are responsible for the observed frequency progressions. This work provides the first evidence for noble gas–actinide complexes, and the first example of neutral complexes with four noble gas atoms bonded to one metal center.

### Introduction

New paradigms in the basic structure and bonding of small actinide-containing molecules have been discovered by combining laser-ablation matrix-infrared experiments with relativistic density functional calculations. Such collaborations have recently identified uranium hydrides, oxides, nitroxides, and carbide-oxides,<sup>1–5</sup> and the thorium analogues.<sup>6–8</sup> In particular, recent reactions of laser-ablated U with CO in excess neon and supporting electronic structure calculations found the linear singlet CUO molecule to be the major primary reaction product followed by linear triplet OUCCO as the major secondary reaction product.<sup>5</sup> Earlier argon matrix U + CO studies gave a different major primary reaction product<sup>9</sup> and the CUO identification in the argon matrix was subsequently questioned<sup>5</sup> owing to the presence of UO and UO<sub>2</sub>, which can also form

carbonyl complexes.<sup>10</sup> The argon matrix experiments were repeated under conditions where UO<sub>2</sub> was virtually absent, and the same argon matrix-isolated CUO species was observed. DFT calculations show that this triplet CUO species is about one kcal/mol higher than singlet CUO in the gas phase, but the matrix experiments trap the triplet species in argon at 7 K and the singlet in neon at 4 K.<sup>11</sup> This rare “ground-state reversal” requires closely spaced low-energy states, which are provided by the actinide CUO molecule, and a specific interaction with argon, which is provided by CUO(Ar)<sub>n</sub> complexes.<sup>12</sup> Analogous CUO(Kr)<sub>n</sub> and CUO(Xe)<sub>n</sub> complexes are formed competitively with 1% Kr and Xe in argon, which suggests the formation of distinct CUO(Ng)<sub>n</sub> complexes as is confirmed by DFT calculations to be reported here.

There are few examples of neutral argon complexes, namely ArW(CO)<sub>5</sub>,<sup>13–15</sup> ArBeO,<sup>16,17</sup> and ArMX (M = Cu, Ag, Au; X = F, Cl),<sup>18–20</sup> and one neutral compound HArF with a strongly covalent (H–Ar)<sup>+</sup> bond<sup>21,22</sup> and a seminal position in noble gas

<sup>†</sup> Department of Chemistry, University of Virginia.

<sup>‡</sup> William R. Wiley Environmental Molecular Sciences Laboratory, Pacific Northwest National Laboratory.

<sup>§</sup> Department of Chemistry, The Ohio State University.

- (1) Souter, P. F.; Kushto, G. P.; Andrews, L.; Neurock, M. *J. Am. Chem. Soc.* **1997**, *119*, 1682.
- (2) Zhou, M. F.; Andrews, L.; Ismail, N.; Marsden, C. *J. Phys. Chem. A* **2000**, *104*, 5495.
- (3) Kushto, G. P.; Souter, P. F.; Andrews, L.; Neurock, M. *J. Chem. Phys.* **1997**, *106*, 5894.
- (4) Zhou, M. F.; Andrews, L. *J. Chem. Phys.* **1999**, *111*, 11 044 (U and Th+NO in neon).
- (5) Zhou, M. F.; Andrews, L.; Li, J.; Bursten, B. E. *J. Am. Chem. Soc.* **1999**, *121*, 9712 (U + CO in neon).
- (6) Souter, P. F.; Kushto, G. P.; Andrews, L.; Neurock, M. *J. Phys. Chem. A* **1997**, *101*, 1287.
- (7) Kushto, G. P.; Andrews, L. *J. Phys. Chem. A* **1999**, *103*, 4836.
- (8) (a) Zhou, M. F.; Andrews, L.; Li, J.; Bursten, B. E. *J. Am. Chem. Soc.* **1999**, *121*, 12188. (b) Li, J.; Bursten, B. E.; Zhou, M. F.; Andrews, L. *Inorg. Chem.* **2001**, *40*, 5448 (Th + CO).
- (9) Tague, T. J., Jr.; Andrews, L.; Hunt, R. D. *J. Phys. Chem.* **1993**, *97*, 10 920.

- (10) Andrews, L.; Zhou, M. F.; Liang, B.; Li, J.; Bursten, B. E. *J. Am. Chem. Soc.* **2000**, *122*, 11 440 (U and Th + CO<sub>2</sub>).
- (11) Andrews, L.; Liang, B.; Li, J.; Bursten, B. E. *Angew. Chem., Int. Ed. Engl.* **2000**, *39*, 4565.
- (12) Li, J.; Bursten, B. E.; Liang, B.; Andrews, L. *Science* **2002**, *295*, 2242.
- (13) Wells, J. R.; Weitz, E. *J. Am. Chem. Soc.* **1992**, *114*, 2783.
- (14) Sun, X.-Z.; George, M. W.; Kazarian, S. G.; Nikiforov, S. M.; Poliakov, M. *J. Am. Chem. Soc.* **1996**, *118*, 10 525.
- (15) Ehlers, A. W.; Frenking, G.; Baerends, E. J. *Organometallics* **1997**, *16*, 4896.
- (16) Thompson, C. A.; Andrews, L. *J. Am. Chem. Soc.* **1994**, *116*, 423.
- (17) Veldkamp, A.; Frenking, G. *Chem. Phys. Lett.* **1994**, *226*, 11.
- (18) Evans, C. J.; Lesarri, A.; Gerry, M. C. L. *J. Am. Chem. Soc.* **2000**, *122*, 6100.
- (19) Evans, C. J.; Gerry, M. C. L. *J. Chem. Phys.* **2000**, *112*, 9363.
- (20) Evans, C. J.; Gerry, M. C. L. *J. Chem. Phys.* **2000**, *112*, 1321.
- (21) Khriachtchev, L.; Pettersson, M.; Runeberg, N.; Lundell, J.; Räsänen, M. *Nature* **2000**, *406*, 874.

chemistry.<sup>23</sup> Hence, the observation and characterization of distinct CUO(Ng) and CUO(Ng)<sub>n</sub> actinide-argon complexes is an important new addition to noble-gas and actinide chemistry.

### Experimental and Computational Methods

The experiment for laser ablation and matrix isolation spectroscopy has been described in detail previously.<sup>24</sup> Briefly, the Nd:YAG laser fundamental (1064 nm, 10 Hz repetition rate with 10 ns pulse width) was focused on the rotating metal uranium or thorium target (Oak Ridge National Laboratory) using low energy (1–5 mJ/pulse) such that a target plume was barely observed. Laser-ablated metal atoms were co-deposited with carbon monoxide (0.2 to 0.4%) in excess argon, krypton, xenon, or argon doped with Kr or Xe onto a 7 K CsI cryogenic window at 2–4 mmol/h for one h. Carbon monoxide (Matheson), <sup>13</sup>C<sup>16</sup>O and <sup>12</sup>C<sup>18</sup>O (Cambridge Isotopic Laboratories), and mixtures were used in different experiments. Infrared spectra were recorded at 0.5 cm<sup>-1</sup> resolution on a Nicolet 550 spectrometer with 0.1 cm<sup>-1</sup> resolution using a HgCdTe detector. Matrix samples were annealed at different temperatures, and selected samples were subjected to broadband photolysis by a medium-pressure mercury arc (Philips, 175W, globe removed, 240–700 nm). Additional experiments were done with CBr<sub>4</sub> added to the sample at 20% of CO concentration to trap laser-ablated electrons and to affect the product chemistry.<sup>25</sup>

Relativistic density functional theory (DFT) calculations have been performed using the Amsterdam Density Functional (ADF 2000) code,<sup>26</sup> with the inclusion of the generalized gradient approach of Perdew and Wang (PW91).<sup>27</sup> This PW91 exchange-correlation functional has recently been shown to be a more reliable choice than other functionals for systems with weak interactions.<sup>28</sup> The [1s<sup>2</sup>] cores for C, O, and Ne, [1s<sup>2</sup>-2p<sup>6</sup>] core for Ar, [1s<sup>2</sup>-3d<sup>10</sup>] core for Kr, [1s<sup>2</sup>-4d<sup>10</sup>] core for Xe, and [1s<sup>2</sup>-5d<sup>10</sup>] core for U were frozen. Slater-type-orbital (STO) basis sets of triple- $\zeta$  quality were used for the valence orbitals of all atoms with d- and f-type polarization functions for the C, O, Ne, Ar, Kr, Xe, and 2s2p2d2f diffuse functions for the noble-gas elements. Numerical integration accuracy of INTEGRATION = 10.0 was used throughout. The structures of the calculated species were fully optimized with the inclusion of scalar (mass-velocity and Darwin) relativistic effects, which were treated within the Pauli formalism via the quasi-relativistic method.<sup>29</sup> Vibrational frequencies were determined via numerical evaluation of the second-order derivatives of the total energies. Owing to the use of very large basis sets, the basis-set-superposition-error is expected to be quite small. Further computational details have been described elsewhere.<sup>30</sup>

### Results

The products of the reaction of laser-ablated uranium atoms with carbon monoxide in solid argon will be identified from the effects of isotopic substitution in their infrared spectra,

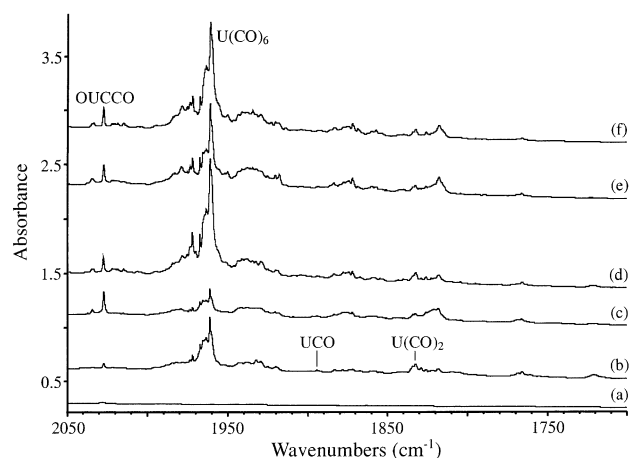


**Figure 1.** Infrared spectra in the 2050–1700 cm<sup>-1</sup> region for laser-ablated U atoms co-deposited with 0.3% CO in argon at 7 K: (a) sample deposited for 70 min, (b) after annealing to 30 K, (c) after  $\lambda > 240$  nm photolysis for 15 min, (d) after annealing to 40 K, (e) after  $\lambda > 240$  nm photolysis for 15 min, and (f) after annealing to 43 K.

comparison to analogous neon matrix absorptions, and DFT calculations. Similar U + CO experiments in krypton, in xenon, and in argon doped with Kr and Xe, and complementary thorium investigations will be compared. We will first show by comparison of frequencies that most of the products are the same in solid neon and argon but that CUO is unique by virtue of its energetically near-degenerate singlet and triplet states and a strong interaction with Ar atoms in the triplet CUO(Ar)<sub>n</sub> complex. We will then examine the bonding and structures of CUO(Ng)<sub>n</sub> ( $n = 1–5$ ) complexes using relativistic DFT calculations.

**OUCCO.** The OUCCO product is common to both neon and argon matrix experiments as demonstrated by a comparison of the observed and DFT calculated frequencies.<sup>5</sup> The strongest OUCCO absorption at 2027.8 cm<sup>-1</sup> in solid argon increases on annealing and photolysis (Figure 1), shifts to 1963.7 cm<sup>-1</sup> with <sup>13</sup>CO, and gives a 2027.8, 2018.2, 1973.8, 1963.7 cm<sup>-1</sup> 1:1:1:1 quartet with <sup>12</sup>CO + <sup>13</sup>CO (Table 1). This band shifts to 2008.8 cm<sup>-1</sup> with <sup>18</sup>O and gives a 2027.8, 2008.8 cm<sup>-1</sup> 1:1 doublet with <sup>16</sup>O + <sup>18</sup>O. The <sup>12</sup>CO/<sup>13</sup>CO isotopic frequency ratio (1.0326) and the <sup>16</sup>O/<sup>18</sup>O ratio (1.0095) show that this is primarily a carbon motion. The mixed carbon isotopic quartet and oxygen isotopic doublet demonstrate that two inequivalent carbon atoms and one oxygen atom participate in this antisymmetric C–C–O stretching mode. The 825.2 cm<sup>-1</sup> band (and 822.2 cm<sup>-1</sup> site) are associated with the 2027.8 cm<sup>-1</sup> band on photolysis and annealing. The 825.2 cm<sup>-1</sup> band shifts to 781.1 cm<sup>-1</sup> with <sup>18</sup>O and the 16/18 ratio (1.0565) and absence of a <sup>13</sup>CO shift are characteristic of a U–O stretching mode. A weak 1352.8 cm<sup>-1</sup> band appears with the 2027.8 and 825.2 cm<sup>-1</sup> bands on annealing and photolysis, and the isotopic shifts are appropriate for a symmetric C–C–O stretching mode.

The 2027.8, 1352.8, and 825.2 cm<sup>-1</sup> argon-matrix bands correspond to bands observed in the neon matrix at 2051.5, 1361.8, and 841.0 cm<sup>-1</sup>. These bands have the same isotopic behavior in both matrices, and correspond reasonably well to the DFT-calculated vibrations at 2125, 1393, and 897 cm<sup>-1</sup> for the linear triplet OUCCO molecule.<sup>5</sup> Thus, it appears that this secondary product is formed by the combination of CO and CUO in both Ne and Ar matrices. Interestingly, however, in

- (22) Runeberg, N.; Pettersson, M.; Khriachtchev, L.; Lundell, J.; Räsänen, M. *J. Chem. Phys.* **2001**, *114*, 836.  
 (23) Pyykkö, P. *Science* **2000**, *290*, 117.  
 (24) (a) Burkholder, T. R.; Andrews, L. *J. Chem. Phys.* **1991**, *95*, 8697. (b) Hassanzadeh, P.; Andrews, L. *J. Phys. Chem.* **1992**, *96*, 9177.  
 (25) (a) Zhou, M.; Andrews, L. *J. Am. Chem. Soc.* **1998**, *120*, 11 499. (b) Zhou, M. F.; Andrews, L. *J. Phys. Chem. A* **1999**, *103*, 2066.  
 (26) ADF 2000.02, SCM, Theoretical Chemistry, Vrije Universiteit, Amsterdam, The Netherlands (<http://www.scm.com>). (a) te Velde, G.; Bickelhaupt, F. M.; van Gisbergen, S. J. A.; Fonseca Guerra, C.; Baerends, E. J.; Snijders, J. G.; Ziegler, T. *J. Comput. Chem.* **2001**, *22*, 931. (b) Fonseca Guerra, C.; Snijders, J. G.; te Velde, G.; Baerends, E. J. *Theor. Chem. Acc.* **1998**, *99*, 391.  
 (27) (a) Perdew, J. P.; Wang, Y. *Phys. Rev. B* **1992**, *45*, 13244. (b) Perdew, J. P.; Chevary, J. A.; Vosko, S. H.; Jackson, K. A.; Pederson, M. R.; Singh, D. J.; Foilhais, C. *Phys. Rev. B* **1992**, *46*, 6671.  
 (28) (a) Wesolowski, T. A.; Parisel, O.; Ellinger, Y.; Weber, J. *J. Phys. Chem. A* **1997**, *101*, 7818. (b) Zhang, Y.; Pan, W.; Yang, W. *J. Chem. Phys.* **1997**, *107*, 7921.  
 (29) Ziegler, T.; Baerends, E. J.; Snijders, J. G.; Ravenek, W. *J. Phys. Chem.* **1989**, *93*, 3050.  
 (30) Li, J.; Bursten, B. E. *J. Am. Chem. Soc.* **1997**, *119*, 9021.

**Table 1.** Infrared Absorptions ( $\text{cm}^{-1}$ ) Observed from Co-deposition of Laser-Ablated U Atoms with CO in Excess Argon at 7 K

$^{12}\text{C}^{16}\text{O}$	$^{13}\text{C}^{16}\text{O}$	$^{12}\text{C}^{18}\text{O}$	$^{12}\text{C}^{16}\text{O}/$ $^{13}\text{C}^{16}\text{O}$	$^{12}\text{C}^{16}\text{O}/$ $^{12}\text{C}^{18}\text{O}$	assignment
3355.0					OUCCO
2138.2	2091.1	2087.1	1.0225	1.0225	CO
2034.7	1970.7	2015.6	1.0325	1.0095	OUCCO site
2027.8 <sup>a</sup>	1963.7	2008.8	1.0326	1.0095	OUCCO
2015.3	1954.4	1994.7	1.0312	1.0100	OUCCO(CO) <sub>x</sub>
1972.4	1930.2	1924.2	1.0219	1.0251	U(CO) <sub>6</sub> site
1961.3	1919.5	1913.2	1.0218	1.0251	U(CO) <sub>6</sub>
1932.6	1890.5	1887.4	1.0219	1.0239	U(CO) <sub>x</sub>
1894.2	1850.7	1850.4	1.0235	1.0237	(UCO)
1872.1	1831.8	1828.9	1.0220	1.0236	U(CO) <sub>x</sub>
1832.6 <sup>b</sup>	1793.6	1788.6	1.0217	1.0246	U(CO) <sub>2</sub>
1818.4	1779.1	1775.3	1.0221	1.0243	U(CO) <sub>x</sub>
1766.0	1728.2	1723.7	1.0219	1.0245	U(CO) <sub>x</sub>
1720.9 <sup>c</sup>	1683.2	1680.2	1.0224	1.0236	U(CO) <sub>x</sub>
1515.5 <sup>d</sup>	1482.2	1479.6	1.0225	1.0243	(CO) <sub>2</sub> <sup>-</sup>
1352.8	1316.7	1320.2	1.0274	1.0247	OUCCO
924.2	891.9	923.3	1.0362	1.0010	CUO <sup>-</sup>
921.1	889.3	920.3	1.0358	1.0009	CUO <sup>-</sup> site
908.6 <sup>e</sup>	908.6	863.1	1.0000	1.0527	(C <sub>2</sub> )UO <sub>2</sub>
852.5	836.8	844.7	1.0188	1.0092	CUO(Ar) <sub>x</sub>
840.8	840.8	796.4	1.0000	1.0558	OU(CO) <sub>x</sub>
834.1	834.1	790.4	1.0000	1.0553	OU(CO) <sub>x</sub>
825.2	825.2	781.1	1.0000	1.0565	OUCCO site
822.2	822.2	778.3	1.0000	1.0564	OUCCO
819.6	819.6	775.8	1.0000	1.0565	UO
804.3	788.8	768.3	1.0196	1.0469	CUO(Ar) <sub>x</sub>
798.1	796.8	755.9	1.0016	1.0558	CUO <sup>-</sup>
796 sh	794 sh	753 sh	1.002	1.057	CUO <sup>-</sup> site

<sup>a</sup> Quartet 2027.8, 2018.2, 1973.8, 1963.9  $\text{cm}^{-1}$  with  $^{12}\text{CO}+^{13}\text{CO}$  and doublet 2027.8, 2008.8  $\text{cm}^{-1}$  with  $\text{C}^{16}\text{O}+\text{C}^{18}\text{O}$ . <sup>b</sup> Triplet at 1832.6, 1820.1, 1793.6  $\text{cm}^{-1}$  with  $^{12}\text{CO}+^{13}\text{CO}$ , and at 1832.6, 1818.7, 1788.6  $\text{cm}^{-1}$  with  $\text{C}^{16}\text{O}+\text{C}^{18}\text{O}$ . <sup>c</sup> Triplet at 1720.9, 1697.7, 1683.2  $\text{cm}^{-1}$  with  $^{12}\text{CO}+^{13}\text{CO}$  and at 1720.9, 1695.4, 1680.2  $\text{cm}^{-1}$  with  $\text{C}^{16}\text{O}+\text{C}^{18}\text{O}$ . <sup>d</sup> Triplet at 1515.5, 1497.4, 1482.2  $\text{cm}^{-1}$  with  $^{12}\text{CO}+^{13}\text{CO}$ . <sup>e</sup> Triplet at 908.6, 892.0, 863.1  $\text{cm}^{-1}$  with  $\text{C}^{16}\text{O}+\text{C}^{18}\text{O}$ .

the Ar experiments there is no analogue to the 1047.3  $\text{cm}^{-1}$  band of CUO that was observed in Ne. The 1000  $\text{cm}^{-1}$  region of the products of U + CO in Ar shows only a trace 1050.8  $\text{cm}^{-1}$  absorption due to UN<sub>2</sub>.<sup>31</sup>

**CUO<sup>-</sup>.** The broad weak bands at 924.2 and 798.1  $\text{cm}^{-1}$  mimic neon-matrix bands at 929.3 and 803.3  $\text{cm}^{-1}$  in their isotopic shifts and frequency ratios (Table 1). The 924.2  $\text{cm}^{-1}$  band is predominantly a U–C vibrational mode whereas the 798.1  $\text{cm}^{-1}$  band is mainly a U–O mode. Both bands appear as doublets in mixed isotopic precursor experiments (Figure 3), so one C and O are involved in argon-matrix product as was the case in neon. Both bands are destroyed by  $\lambda > 470$  nm photolysis. Experiments with electron-trapping reagents also provide strong evidence that these bands are due to an anionic species. Normally, we employ CCl<sub>4</sub> dopant to capture electrons and to prevent the formation of product anions.<sup>2,12,13</sup> However, inasmuch as CCl<sub>4</sub> and its photolysis products mask the 925 and 800  $\text{cm}^{-1}$  regions, we used CBr<sub>4</sub> for these studies because the CBr<sub>4</sub>, CBr<sub>3</sub>, and CBr<sub>3</sub><sup>+</sup> absorptions appear at lower frequencies.<sup>32</sup> Doping the argon with CBr<sub>4</sub> reduces the intensities of the 924.2 and 798.1  $\text{cm}^{-1}$  bands more than 10-fold relative to the 852.5 and 804.3  $\text{cm}^{-1}$  absorptions. The (CO)<sub>2</sub><sup>-</sup> anion also failed to appear in the presence of CBr<sub>4</sub>.<sup>13,14</sup> We previously assigned the neon-matrix bands to the CUO<sup>-</sup> anion on the basis of their isotopic shifts and agreement with DFT frequencies

(31) Hunt, R. D.; Yustein, J. T.; Andrews, L. *J. Chem. Phys.* **1993**, *98*, 6070.  
(32) Prochaska, F. T.; Andrews, L. *J. Chem. Phys.* **1977**, *67*, 1091.

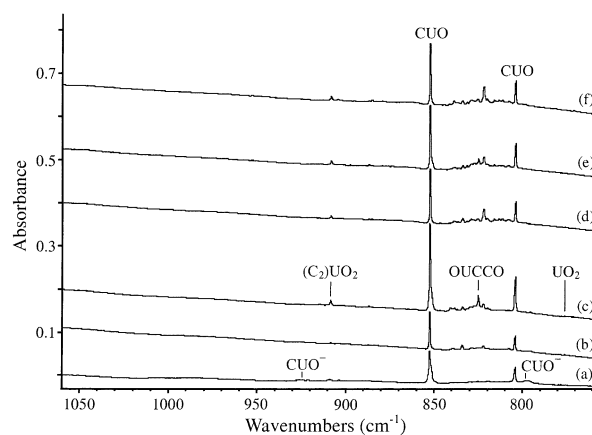


**Figure 2.** Infrared spectra in the 1060–760  $\text{cm}^{-1}$  region for laser-ablated U atoms co-deposited with 0.3% CO in argon at 7 K: (a) sample deposited for 70 min, (b) after annealing to 30 K, (c) after  $\lambda > 240$  nm photolysis for 15 min, (d) after annealing to 40 K, (e) after  $\lambda > 240$  nm photolysis for 15 min, and (f) after annealing to 43 K.

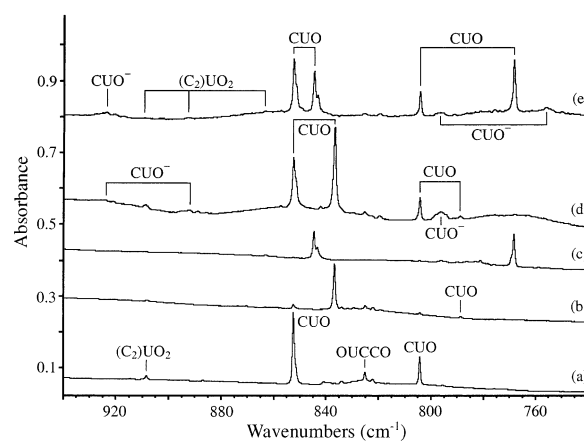


**Figure 3.** Infrared spectra in the 940–740  $\text{cm}^{-1}$  region for laser-ablated U atoms co-deposited with isotopic CO in argon: (a) 0.3%  $^{12}\text{CO}$  after deposition and  $\lambda > 240$  nm photolysis, (b) 0.2%  $^{13}\text{CO}$  after deposition and  $\lambda > 240$  nm photolysis, (c) 0.3%  $\text{C}^{18}\text{O}$  after deposition and  $\lambda > 240$  nm photolysis, (d) 0.2%  $^{12}\text{CO}$  + 0.2%  $^{13}\text{CO}$  after deposition, and (e) 0.2%  $\text{C}^{16}\text{O}$  + 0.2%  $\text{C}^{18}\text{O}$  after deposition.

calculated for bent CUO<sup>-</sup> at 996 and 822  $\text{cm}^{-1}$ . The 924.2 and 798.1  $\text{cm}^{-1}$  bands in the argon matrix are therefore assigned to the same bent CUO<sup>-</sup> species with further support by marked decrease in the presence of a strong electron-trapping molecule. This assignment leads to an intriguing question: Where in the spectrum is the CUO species that must capture electrons to form CUO<sup>-</sup>?

**Triplet CUO in Argon.** The strongest bands observed following the reaction of U with CO in argon are those at 852.5 and 804.3  $\text{cm}^{-1}$ . This result is in agreement with our previous experiments in an argon matrix,<sup>9</sup> but these bands are substantially different from those at 1047.3 and 872.2  $\text{cm}^{-1}$ , which dominate the neon-matrix results and were assigned to linear, singlet CUO.<sup>5</sup> Nevertheless, several aspects of the argon-matrix experiments make for a compelling case that the 852.5 and 804.3  $\text{cm}^{-1}$  bands are due to the CUO moiety. First, we note the virtual absence of UO and UO<sub>2</sub> from the present infrared spectra, so atomic uranium is the primary agent for reaction with CO. Indeed, the experiments with isotopomers of CO lead to mixed isotopic doublets for the 852.5 and 804.3  $\text{cm}^{-1}$  bands [Figure 3d,e], demonstrating that single C and O atoms are involved in



these two vibrational modes. Note the detailed annealing and photolysis spectra in Figure 2, which clearly associates these two bands with a common molecule. On annealing to 25 K, the two bands sharpen but the integrated intensities slightly decrease. The bands increase in concert on photolysis with  $\lambda > 470, 290,$  and  $240$  nm radiation in different experiments. Just as found for linear singlet CUO absorbing at 1047.3 and 872.2  $\text{cm}^{-1}$  in neon,<sup>5</sup> the present CUO species does not form from cold U and CO, but laser-ablated U or mercury arc irradiated U react with CO to form the new species absorbing at 852.5 and 804.3  $\text{cm}^{-1}$  in solid argon.

Typical neon-to-argon red shifts for small heavy metal species include 7.4  $\text{cm}^{-1}$  for HfO,<sup>33</sup> 8.3  $\text{cm}^{-1}$  for ThO,<sup>4,8,34,35</sup> 23.9 and 12.5  $\text{cm}^{-1}$  for NThO,<sup>4,35</sup> and 19.0 and 11.7  $\text{cm}^{-1}$  for bent triplet CThO (see below).<sup>8</sup> The 194.8 and 67.9  $\text{cm}^{-1}$  neon-to-argon red shifts observed here for CUO are far too large for a solvent polarizability effect normally known as the “matrix shift.”<sup>36</sup> Hence, we must find another explanation for the markedly different CUO frequencies.

Relativistic DFT calculations were used to characterize another CUO species that might be compatible with the above observations. Because CUO only has three atoms, it can only have four different isomers, i.e., CUO, UCO, UOC, and (U- $\eta^2$ -CO). Our calculations indicate UCO, UOC, and the side-bound (U- $\eta^2$ -CO) organoactinide complexes in triplet and quintet states are much higher in energy than singlet linear CUO. These molecules also have very different vibrational spectra than observed in solid argon. Therefore, the spectra are due to the CUO molecule in a different electronic state. Our calculations indicate that the CUO molecule is unique in that it has a low-lying triplet state only about 1 kcal/mol higher in energy than the  $^1\Sigma^+$  ground state of linear CUO. This triplet state has stretching frequencies calculated at 902  $\text{cm}^{-1}$  (311 km/mol intensity) and 843  $\text{cm}^{-1}$  (115 km/mol). These calculated frequencies are 5.8% and 4.8% higher than those of the argon-matrix product bands and match the observed 3/1 relative intensity ratio quite well. The calculated pure singlet state CUO frequencies are each 0.2% higher than the neon matrix observations, which is in much better agreement, but the matrix interaction and shift are typically greater for argon than for neon.<sup>36</sup> As will be detailed later in this paper, a specific interaction of Ar atoms in the matrix with the CUO molecule is sufficient to make the triplet form of a complex of CUO with Ar atoms (hereafter denoted CUO(Ar)<sub>n</sub>) lower than that for singlet CUO(Ar)<sub>n</sub>.<sup>11</sup> To understand the basis for this unusual “matrix interaction” (or “ground-state reversal”), additional DFT calculations were performed on discrete molecular complexes of CUO with a varying number of Ar atoms. For the  $^3A''$  state of the “mono-argon adduct” CUO(Ar), the calculated C–U and U–O stretching frequencies are 887  $\text{cm}^{-1}$  (260 km/mol) and 834  $\text{cm}^{-1}$  (137 km/mol). These calculated frequencies, which are respectively 15 and 9  $\text{cm}^{-1}$  lower than those of isolated triplet CUO, are closer to the observed bands. The complexation of additional Ar atoms to CUO leads to a further decrease in the calculated frequencies; for the triplet  $C_{4v}$  CUO(Ar)<sub>4</sub> complex,

**Table 2.** Observed and Calculated Frequencies ( $\text{cm}^{-1}$ ) and Isotopic Frequency Ratios for the Bond Stretching Modes of CUO and CUO(Ng) Complexes

experimental			calculated (relativistic DFT)		
$\nu_{\text{obs}}$	$^{12}\text{C}/^{13}\text{C}$	$^{16}\text{O}/^{18}\text{O}$	$\nu_{\text{calc}}$	$^{12}\text{C}/^{13}\text{C}$	$^{16}\text{O}/^{18}\text{O}$
Ne matrix			CUO ( $^1\Sigma^+$ )		
872.2	1.0020	1.0554	874	1.0023	1.0549
1047.3	1.0361	1.0010	1049	1.0357	1.0019
			CUO ( $^3\Phi$ )		
			843	1.0127	1.0514
			902	1.0260	1.0052
Ar matrix			CUO(Ar) ( $^3A''$ )		
804.3	1.0196	1.0469	834	1.0125	1.0520
852.5	1.0188	1.0092	887	1.0260	1.0045
			CUO(Kr) ( $^3A''$ )		
803.1			832	1.0140	1.0512
851.0			885	1.0247	1.0076
			CUO(Xe) ( $^3A''$ )		
801.3	1.0202	1.0466	830	1.0155	1.0506
848.0	1.0181	1.0095	879	1.0233	1.0061

which will be discussed later, the frequencies are reduced another 12 and 8  $\text{cm}^{-1}$  more, respectively, and are closer still to the observed bands.

In addition to  $^{12}\text{C}^{16}\text{O}$  frequencies, the  $^{13}\text{C}^{16}\text{O}$  and  $^{12}\text{C}^{18}\text{O}$  isotopic frequencies were also calculated as a diagnostic for the normal mode description. As can be seen in Table 2, the calculated vs observed isotopic frequency ratios are in very near agreement ( $\pm 0.4$   $\text{cm}^{-1}$  discrepancy for the major shifts of 36.5 and 45.8  $\text{cm}^{-1}$ ) for the singlet linear species, but agreement for the triplet is not as good (the major calculated shifts of 15.7 and 36.0  $\text{cm}^{-1}$  are too high by 7 and 3  $\text{cm}^{-1}$ , respectively). The calculated relative intensities are qualitatively correct for the upper and lower triplet CUO bands: the observed integrated intensity ratios 3.2/1.0 vs 1.8/1.0 (calcd) for  $^{12}\text{C}^{16}\text{O}$ , 12/1 vs 22/1 (calcd) for  $^{13}\text{C}^{16}\text{O}$ , and 1.1/1.0 vs 1.8/1.0 (calcd) for  $^{12}\text{C}^{18}\text{O}$ .

The computed displacement coordinates show that the calculated 887  $\text{cm}^{-1}$  band of triplet CUO(Ar) is an antisymmetric stretching mode with 2.5 times more carbon than oxygen displacement and the calculated 834  $\text{cm}^{-1}$  band is a symmetric stretching mode with 1.7 times more oxygen than carbon motion. The observed isotopic shifts demonstrate that there is considerably more mode mixing in the triplet CUO(Ar)<sub>n</sub> complex, where the two bond stretching frequencies are much closer (48.2  $\text{cm}^{-1}$  separation) than for singlet CUO (175.1  $\text{cm}^{-1}$  separation). For singlet CUO in neon, the 1047.3  $\text{cm}^{-1}$  band shifted 36.5  $\text{cm}^{-1}$  with  $^{13}\text{CO}$  and 1.0  $\text{cm}^{-1}$  with  $\text{C}^{18}\text{O}$ , and the 872.2  $\text{cm}^{-1}$  absorption shifted 1.7  $\text{cm}^{-1}$  with  $^{13}\text{CO}$  and 45.8  $\text{cm}^{-1}$  with  $\text{C}^{18}\text{O}$ . In contrast for triplet CUO in argon, the 852.5  $\text{cm}^{-1}$  band shifted 15.7  $\text{cm}^{-1}$  with  $^{13}\text{CO}$  and 7.8  $\text{cm}^{-1}$  with  $\text{C}^{18}\text{O}$ , and the 804.3  $\text{cm}^{-1}$  absorption shifted 15.5  $\text{cm}^{-1}$  with  $^{13}\text{CO}$  and 36.0  $\text{cm}^{-1}$  with  $\text{C}^{18}\text{O}$ . In addition, because the argon atoms interact most strongly with the U and C atoms and the U–C bond order is reduced in triplet CUO, the U–C stretching frequency is affected much more than the U–O frequency relative to the CUO molecule isolated in solid neon.

(C<sub>2</sub>)UO<sub>2</sub>. Ultraviolet photolysis in the neon matrix experiments produced the lowest energy UC<sub>2</sub>O<sub>2</sub> isomer, ( $\eta^2$ -C<sub>2</sub>)UO<sub>2</sub>, which was observed from its UO<sub>2</sub> stretching modes at 922.1 and 843.2  $\text{cm}^{-1}$ .<sup>5</sup> The higher-energy mode is red-shifted in solid argon to 908.6  $\text{cm}^{-1}$ , which is a typical matrix shift. We were unable to observe the lower-energy O–U–O stretching mode

(33) Chertihin, G. V.; Andrews, L. J. *Phys. Chem.* **1995**, *99*, 6356 and unpublished results on HfO in solid neon at 965.7  $\text{cm}^{-1}$ .

(34) Gablenick, S. D.; Reedy, G. T.; Chasanov, M. G. *J. Chem. Phys.* **1974**, *60*, 1167 (ThO in argon).

(35) Kushto, G. P.; Andrews, L. J. *Phys. Chem. A* **1999**, *103*, 4836 (ThO, NThO in argon).

(36) Jacox, M. E. *Chem. Phys.* **1994**, *189*, 149.

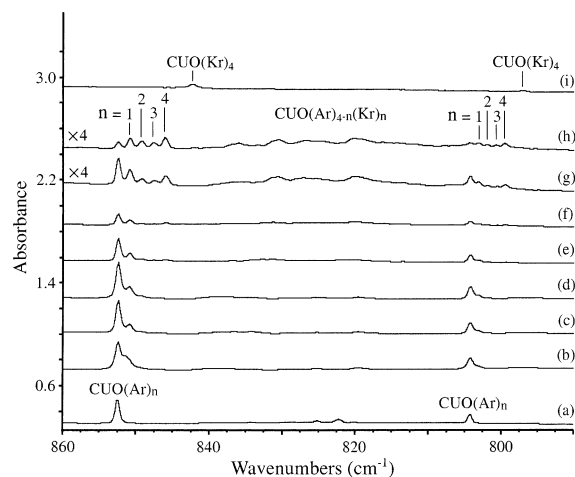


**Figure 4.** Infrared spectra in the 860–780  $\text{cm}^{-1}$  region for CUO formed by laser-ablated U and CO reaction in excess argon: (a) 0.3% CO in pure argon after sample deposition at 7 K, (b) 0.3% CO, 2% Kr in argon after deposition at 7 K, (c) after annealing to 30 K, (d) after full-arc photolysis, (e) after annealing to 45 K, (f) after annealing to 48 K, (g) after annealing to 50 K (intensity  $\times 4$ ), (h) after annealing to 52 K (intensity  $\times 4$ ), and (i) 0.4% CO in pure krypton after deposition at 7 K.

in the argon matrix. The involvement of two CO submolecules in the reaction and two equivalent O atoms in the product is confirmed by the 908.6, 892.0, 863.1  $\text{cm}^{-1}$  1:2:1 triplet observed with a  $\text{C}^{16}\text{O}/\text{C}^{18}\text{O}$  mixture.

**U(CO)<sub>x</sub>.** The present argon-matrix experiments add some information on uranium carbonyl complexes. The very strong 1961.3–1919.5  $\text{cm}^{-1}$  and 1961.3–1913.2  $\text{cm}^{-1}$  doublets for mixed isotopic precursors after extensive annealing are in accord with those expected for the triply degenerate mode for an octahedral complex.<sup>37</sup> We therefore propose that this final product after annealing is  $\text{U}(\text{CO})_6$ , in agreement with previous authors.<sup>38</sup> The observed 1832.6  $\text{cm}^{-1}$  band in argon is just below the 1840.2  $\text{cm}^{-1}$  band observed in neon. We previously proposed that this band is due to the symmetric C–O stretching mode of  $\text{U}(\text{CO})_2$  in solid neon, and the triplet mixed isotopic spectra support a like assignment in solid argon. The weak 1894.2–1850.7  $\text{cm}^{-1}$  doublet is probably due to  $\text{UCO}$ .<sup>5</sup> In  $^{12}\text{CO}_2/^{13}\text{CO}_2$  experiments,<sup>10</sup> a major product identified as  $\text{O}_2\text{UCO}$  absorbs at 1893.4–1851.0  $\text{cm}^{-1}$  so this product must be considered here; however, the virtual absence of  $\text{UO}_2$  casts doubt on the latter possibility.

**U + CO Reaction Products in Argon Doped with Kr and Xe.** To explore further the interactions of noble-gas atoms with CUO, additional experiments were done in which the argon carrier gas is doped with Kr or Xe. For example, an experiment was done in which laser-ablated U atoms were generated with 0.3% CO and 1% Kr in argon. The same products observed in pure Ar were observed as described above. In addition, new features were observed near the 852.5 and 804.3  $\text{cm}^{-1}$  bands assigned to  $\text{CUO}(\text{Ar})_n$ . In particular, new bands appeared at 850.9 and 803.1  $\text{cm}^{-1}$ , and very weak features appeared at 849.3 and 801.8  $\text{cm}^{-1}$  on annealing. Another experiment with 2% Kr in argon and more extensive annealing yields the spectra shown in Figure 4. This figure also shows spectra in pure argon and in pure krypton [Figure 4a,i], which form the boundaries for

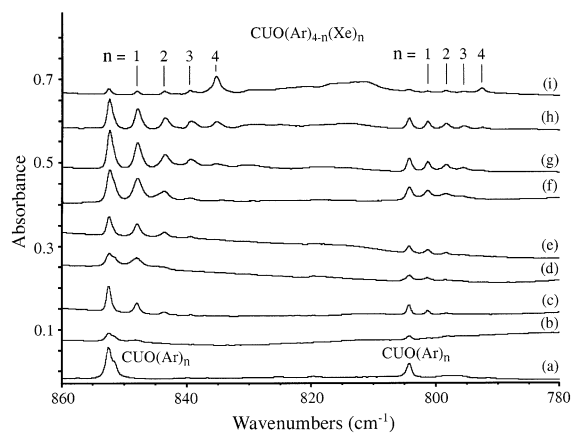


**Figure 5.** Infrared spectra in the 860–780  $\text{cm}^{-1}$  region for CUO formed by laser-ablated U and CO reaction in excess argon: (a) 0.3% CO in pure argon after sample deposition at 7 K, (b) 0.2% CO, 1% Xe in argon after deposition at 7 K, (c) after annealing to 40 K, (d) 0.2% CO, 2% Xe in argon after deposition at 7 K, (e) after annealing to 40 K, (f) 0.2% CO, 3% Xe in argon after deposition at 7 K, (g) after annealing to 40 K, (h) after annealing to 45 K, and (i) after annealing to 50 K.

**Table 3.** Comparison of Neon, Argon, and Krypton Matrix Frequencies ( $\text{cm}^{-1}$ ) Observed for Major Uranium and Thorium Carbon Monoxide Reaction Products

molecule	neon	argon	krypton	xenon
OUCCO	2051.5	2027.8	2021.4	2012.1
	841.0	825.2	826.7	814.3
$\text{U}(\text{CO})_2$	1840.2	1832.6	(1824.3)	
$\text{U}(\text{CO})_6$	(1959.5)	1961.3	1964.5	
UCO	(1917.8)	(1894.2)	(1886.2)	
UO	889.5	819.6	819.0	
$\text{CUO} (^1\Sigma^+)$	1047.3			
	872.2			
$\text{CUO}(\text{Ng})_n (^3A'')$		852.5	842.3	829.8
		804.3	797.1	789.2
OThCCO	2048.6	2024.0	2020.2	
	822.5	804.2	803.8	
$\text{Th}(\text{CO})_2$	1827.7	1787.6	1780.4	
	1775.6	1716.6	1704.1	
$\text{Th}(\text{CO})_6$	1999.7	1980.5	1976.7	
ThCO	1817.5	1800.8	1792.2	
ThO	887.1	876.5	874.2	
	812.2	793.2	784.6	
$\text{CThO}(\text{Ng})_n (^3A')$	617.7	606.0	596.1	

mixed complexes. Upon annealing, two progressions of new bands below the pure-argon bands evolve at 850.9, 849.3, 847.6, 846.0  $\text{cm}^{-1}$  and at 803.1, 801.8, 800.6, 799.4  $\text{cm}^{-1}$  [Figure 4b–h]. After annealing to 52 K, the last bands in the progressions become stronger than the initial pure argon bands at 852.5 and 804.3  $\text{cm}^{-1}$  and the band positions approach those of the major product in pure krypton at 842.3 and 797.1  $\text{cm}^{-1}$ .

Five U + CO experiments were done with Xe in argon, and Figure 5 illustrates representative spectra starting with the pure argon reference [Figure 5a]. With 0.2% CO and 1% Xe, distinct new absorptions were observed at 848.0 and 801.3  $\text{cm}^{-1}$ , and new bands at 843.5 and 798.3  $\text{cm}^{-1}$  appeared on annealing [Figure 5b,c]. With 2% Xe in argon, the latter bands were much stronger and new bands appeared at 839.4, 835.4  $\text{cm}^{-1}$  and at 795.5, 792.6  $\text{cm}^{-1}$ . A sequence of annealing and  $\lambda > 240 \text{ nm}$  irradiation cycles increased the intensities of the new features until they ultimately reach the total intensity observed in pure argon [Figure 5d,e]. The observation that only 2% Xe in argon is enough to cause half of the total absorbance to be due to the

(37) Darling, J. H.; Ogden, J. S. *J. Chem. Soc., Dalton Trans.* **1972**, 2496.

(38) Slater, J. L.; Sheline, R. K.; Lin, K. C.; Weltner, W., Jr. *J. Chem. Phys.* **1971**, 55, 5129.

**Table 4.** Infrared Absorptions ( $\text{cm}^{-1}$ ) for CUO in Various Solid Noble-Gas Environments

Ng	U–C mode <sup>a</sup>	U–O mode <sup>a</sup>
Ne	1047.3	872.2
Ar	852.5	804.3
Kr	842.3	797.1
Xe	829.8 <sup>b</sup>	789.2 <sup>b</sup>
Ne, 1% Ar	1047.3, 857.2, 854.3	872.2, 808.3, 806.4
Ar, 1% Kr	852.5, 850.9, 849.3, 847.6, 846.0 <sup>c</sup>	804.3, 803.1, 801.8, 800.6, 799.4 <sup>c</sup>
	[844.7, 843.1, 841.5, 839.8, 838.2] <sup>d</sup>	[768.3, 767.2, 766.0, 764.8, 763.7] <sup>d</sup>
Ar, 1% Xe	852.5, 848.0, 843.6, 839.4, 835.4 <sup>e</sup>	804.3, 801.3, 798.4, 795.5, 792.6 <sup>e</sup>
	[844.7, 840.0, 835.6, 831.4] <sup>d</sup>	[768.3, 765.6, 763.0, 760.3] <sup>d</sup>
	[836.8, 832.9, 829.1, 825.2, 822.0] <sup>f</sup>	[788.8, 786.8, 785.4] <sup>f</sup>
Kr, 2% Xe	842.3, 839.7, 837.2, 834.7, 832.2	797.1, 795.4, 793.8, 792.1, 790.5

<sup>a</sup> Dominant internal coordinate in the stretching mode. <sup>b</sup> Major site in pure xenon. <sup>c</sup> Last two bands observed with Ar, 2% Kr. <sup>d</sup> Absorptions for  $^{12}\text{C}^{18}\text{O}$ . <sup>e</sup> Last band observed with Ar, 2% Xe; latter bands stronger with Ar, 3% Xe. <sup>f</sup> Absorptions for  $^{13}\text{C}^{16}\text{O}$ .

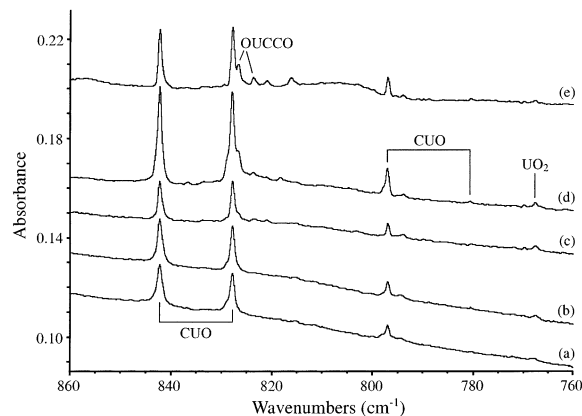
new features makes it evident that the Xe atoms interact with the product molecule preferentially over the Ar atoms. With 3% Xe in argon, the satellite progressions are much stronger, and after 50 K annealing the final 835.4 and 792.6  $\text{cm}^{-1}$  bands dominate the product spectrum.

Table 4 summarizes the new product absorptions, and highlights several trends. First, from the spectra of CUO in pure Ar, Kr, or Xe, we see that the vibrational bands of the  $\text{CUO}(\text{Ng})_n$  species show substantial red-shifts from Ar to Kr to Xe: Relative to the 852.5 and 804.3  $\text{cm}^{-1}$  bands of  $\text{CUO}(\text{Ar})_n$ , the bands of  $\text{CUO}(\text{Kr})_n$  are red-shifted by 10.2 and 7.2  $\text{cm}^{-1}$ , respectively, and those of  $\text{CUO}(\text{Xe})_n$  are shifted by 22.7 and 15.1  $\text{cm}^{-1}$ . Second, the experiments in which argon is doped with Kr or Xe show that the first  $\text{CUO}(\text{Kr})$  and  $\text{CUO}(\text{Xe})$  species in solid argon show small red-shifts (1.5 and 1.2  $\text{cm}^{-1}$  for Kr; 4.5 and 3.0  $\text{cm}^{-1}$  for Xe) compared to  $\text{CUO}(\text{Ar})_n$ . Third, the four-band progressions below the bands of  $\text{CUO}(\text{Ar})_n$  when Kr and Xe are doped into argon strongly suggest the successive formation of distinct  $\text{CUO}(\text{Ng})_n$  ( $\text{Ng} = \text{Kr}, \text{Xe}; n = 1, 2, 3, 4$ ) complexes. The observation of four distinct Kr and four distinct Xe complex species provides strong evidence that four heavy Ng (Ar, Kr, Xe) atoms complex with U in the intimate shell around triplet CUO. These results suggest that the progressions result from the successive replacement of coordinated Ar atoms with Kr or Xe atoms, so we propose the formation of a series of six-coordinate  $\text{CUO}(\text{Ar})_{4-n}(\text{Ng})_n$  ( $\text{Ng} = \text{Kr}, \text{Xe}; n = 1, 2, 3, 4$ ) complexes.

The  $^{13}\text{C}^{16}\text{O}$  and  $^{12}\text{C}^{18}\text{O}$  isotopic frequencies show that the normal modes of  $\text{CUO}(\text{Ar})_3(\text{Xe})$  are almost the same as for  $\text{CUO}(\text{Ar})_n$ . The  $^{12}\text{C}^{16}\text{O}/^{13}\text{C}^{16}\text{O}$  and  $^{12}\text{C}^{16}\text{O}/^{12}\text{C}^{18}\text{O}$  frequency ratios for the 848.0  $\text{cm}^{-1}$  (1.0181 and 1.0202) and 801.3  $\text{cm}^{-1}$  (1.009 52 and 1.0466) bands can be compared with the values for  $\text{CUO}(\text{Ar})_n$  in Table 1. Isotopic frequency ratios for the 843.6 and 798.4  $\text{cm}^{-1}$  bands of  $\text{CUO}(\text{Ar})_2(\text{Xe})_2$  (1.0175, not observed and 1.009 57, 1.0464) and for the 839.4 and 795.5  $\text{cm}^{-1}$  bands  $\text{CUO}(\text{Ar})(\text{Xe})_3$  (1.0172, not observed and 1.009 62, 1.0463) continue the slight trend of decreasing carbon and increasing oxygen participation in the upper (mostly U–C) mode and increasing carbon and decreasing oxygen participation in the lower (mostly U–O) mode with increasing number of Xe atoms.

#### U + CO Reaction Products in Solid Krypton and Xenon.

When laser-ablated uranium atoms were reacted with 0.4% CO in krypton, the major product on deposition has absorptions at 842.3 and 797.1  $\text{cm}^{-1}$ . These bands were unchanged on annealing to 25 and 35 K, but weak new bands at 1886.2, 1824.3, and 1758.2  $\text{cm}^{-1}$  increased in intensity. Photolysis ( $\lambda$



**Figure 6.** Infrared spectra in the 860–760  $\text{cm}^{-1}$  region for laser-ablated U atoms co-deposited with 0.4%  $^{12}\text{C}^{18}\text{O}$  + 0.4%  $^{13}\text{C}^{16}\text{O}$  in krypton at 7 K: (a) sample deposited for 40 min, (b) after annealing to 25 K, (c) after annealing to 35 K, (d) after  $\lambda > 470$  nm photolysis for 30 min, and (e) after annealing to 40 K.

$> 470$  nm) reduced the latter bands, tripled the former bands and increased the intensity of bands at 2021.4 and 826.7  $\text{cm}^{-1}$  10-fold. Further annealing to 40 and 50 K reduced the intensities of all these bands and produced a very strong 1964.5  $\text{cm}^{-1}$  absorption. Table 3 compares the frequencies observed in the krypton matrix, which are shifted only slightly from those in the argon matrix.

Figure 6 shows the spectra that result from the reaction of U atoms with a  $^{12}\text{C}^{16}\text{O}/^{13}\text{C}^{16}\text{O}$  mixture in krypton. The doublets at 842.3–827.9  $\text{cm}^{-1}$  and 797.1–780.6  $\text{cm}^{-1}$  confirm that this product requires a single CO molecule; it is clearly the krypton-matrix counterpart of CUO in solid argon. The  $^{12}\text{C}^{16}\text{O}/^{13}\text{C}^{16}\text{O}$  ratios, 1.0174 and 1.0210, are almost the same as the argon matrix values. Annealing had no effect but photolysis ( $\lambda > 470$  nm) again tripled these bands in concert. The 2021.4  $\text{cm}^{-1}$  band gave a quartet absorption with additional peaks at 2011.5, 1968.3, and 1957.0  $\text{cm}^{-1}$ . The 1824.3  $\text{cm}^{-1}$  band is probably due to  $\text{U}(\text{CO})_2$ , and the 1758.2  $\text{cm}^{-1}$  absorption arises from a higher carbonyl. After annealing a strong, broad doublet was observed at 1964.5–1924.5  $\text{cm}^{-1}$ , consistent with the presence of  $\text{U}(\text{CO})_6$ .

Experiments were also performed in which U atoms reacted with 0.2–0.5% CO in pure xenon. The CUO molecule apparently can sit in two different sites within the matrix, with absorptions at 834.6 and 797.2  $\text{cm}^{-1}$  (Site 1) and at 829.8 and 789.2  $\text{cm}^{-1}$  (Site 2). Annealing the matrix favors the peaks for Site 2. On the basis of the results in the Xe-doped Ar and Kr matrices, it seems likely that the dominant species is  $\text{CUO}(\text{Xe})_4$ .



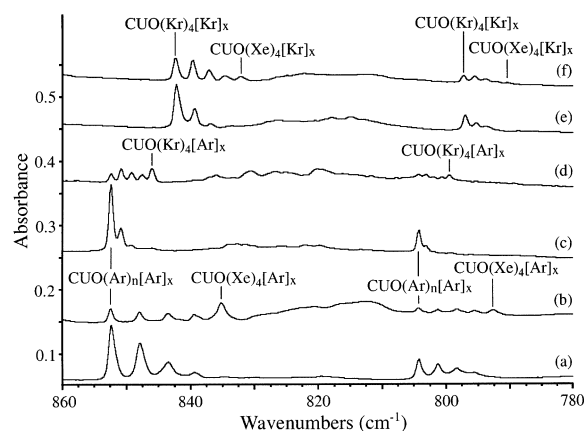


**Figure 7.** Infrared spectra in the 860–780  $\text{cm}^{-1}$  region for CUO formed by laser-ablated U and CO reaction in mixed noble gas samples: (a) 0.2% CO, 3% Xe in argon after deposition at 7 K, photolysis and annealing to 30 K (b) after annealing to 48 K, (c) 0.5% CO, 2% Kr in argon after deposition at 7 K, photolysis and annealing to 43 K, (d) after annealing to 52 K, (e) 0.2% CO, 3% Xe in krypton after deposition at 7 K, photolysis and annealing to 40 K, and (f) after annealing to 60 K.

Note in Table 4 that there is a gradual matrix-induced red-shift of the peaks assigned to CUO(Xe)<sub>4</sub> when produced via Xe doping in Ar (835.4 and 792.6  $\text{cm}^{-1}$ ), Xe doping in Kr (832.2 and 790.5  $\text{cm}^{-1}$ ) and in pure Xe (829.8 and 789.2  $\text{cm}^{-1}$ ).

**U + CO Reaction Products in Krypton Doped with Xe.** Several experiments were done with U atoms, CO and 2–3% Xe in krypton. In addition to the bands observed in pure krypton at 842.3 and 797.1  $\text{cm}^{-1}$ , new four-band progressions at 839.7, 837.2, 834.7, 832.2 and 795.4, 793.8, 792.1, 790.5  $\text{cm}^{-1}$  increased on successive annealing cycles. These progressions are due to CUO(Kr)<sub>4-n</sub>(Xe)<sub>n</sub> complexes. Figure 7 contrasts later annealing cycles for Xe in krypton with spectra for Kr in argon and Xe in argon. In each case we see progressions that show the successive replacement of lighter noble-gas atoms with heavier ones upon annealing.

**Complementary Th + CO Species.** We have previously reported properties of the CThO molecule, which results from the reaction of laser-ablated Th atoms with CO in neon.<sup>8</sup> Like CUO, CThO is the result of the insertion of an actinide atom into the CO triple bond. However, because Th has two fewer valence electrons than U, CThO has significant electronic and structural differences with CUO. For the present studies, we have prepared CThO in solid argon for comparison with the results in a neon matrix. Table 5 lists the observed frequencies of CThO in solid argon. Figure 8 shows the infrared spectra of the products of the reaction between Th atoms and <sup>12</sup>CO/<sup>13</sup>CO and C<sup>16</sup>O/C<sup>18</sup>O mixtures. The strong 793.2–751.2  $\text{cm}^{-1}$  doublet observed with the C<sup>16</sup>O/C<sup>18</sup>O mixture indicates a single Th–O stretching mode [Figure 8d,e,f]. Likewise, the medium intensity 606.0–583.8  $\text{cm}^{-1}$  doublet observed with the <sup>12</sup>CO/<sup>13</sup>CO mixture is characteristic of a single Th–C stretch [Figure 8a,b,c]. These bands are associated with the same molecule by their growth in concert on  $\lambda > 470$  and 290 nm irradiation and their decreases on annealing reacting with CO to form OThCCO. The 793.2 and 606.0  $\text{cm}^{-1}$  bands exhibit almost the same C<sup>16</sup>O/C<sup>18</sup>O (1.0559) and <sup>12</sup>CO/<sup>13</sup>CO (1.0380) isotopic frequency ratios, respectively, as the 812.2 and 617.7  $\text{cm}^{-1}$  bands in the neon matrix bands (1.0559 and 1.0382). We previously assigned the bands in the neon matrix to CThO and used DFT to predict

**Table 5.** Infrared Absorptions ( $\text{cm}^{-1}$ ) from Co-deposition of Laser-Ablated Th Atoms with CO in Excess Argon at 7 K

<sup>12</sup> C <sup>16</sup> O	<sup>13</sup> C <sup>16</sup> O	<sup>12</sup> C <sup>18</sup> O	<sup>12</sup> C <sup>16</sup> O/ <sup>13</sup> C <sup>16</sup> O	<sup>12</sup> C <sup>16</sup> O/ <sup>12</sup> C <sup>18</sup> O	assignment
2034.5		2016.3		1.0090	OThCCO site
2024.0	1959.8 <sup>a</sup>	2005.4	1.0328	1.0093	OThCCO site
2023.0	1959.1 <sup>b</sup>	2004.5	1.0326	1.0092	OThCCO
1974.2	1932.8	1925.8	1.0214	1.0251	Th(CO) <sub>6</sub>
1972.3	1930.8	1924.1	1.0215	1.0251	Th(CO) <sub>6</sub> site
1935.2					?
1889.4					?
1872.7	1833.8		1.0212		?
1806.1	1766.5	1763.4	1.0224	1.0242	ThCO site
1800.8	1761.3	1758.6	1.0224	1.0240	ThCO site
1797.6	1758.2	1755.5	1.0224	1.0240	ThCO
1787.6	1748.0 <sup>c</sup>	1746.0 <sup>d</sup>	1.0227	1.0238	Th(CO) <sub>2</sub> sym
1772.1	1736.8	1732.1	1.0221	1.0248	Th(CO) <sub>2</sub> site
1724.3	1687.3 <sup>e</sup>	1682.3 <sup>f</sup>	1.0219	1.0250	Th(CO) <sub>2</sub> site
1716.7	1678.9 <sup>g</sup>	1676.4 <sup>h</sup>	1.0225	1.0240	Th(CO) <sub>2</sub> antisym
1515.5	1482.3	1479.6	1.0224	1.0243	(CO) <sub>2</sub> <sup>-</sup>
1342.2					OThCCO
878.8	878.8	832.0	1.0000	1.0563	ThO site
876.4	876.4	829.7	1.0000	1.0563	ThO
804.2	804.2	761.3	1.0000	1.0564	OThCCO
793.2	792.9	751.2	1.0003	1.0559	CThO
748.8	748.2	709.4	1.0008	1.0555	CThO <sup>-</sup>
729.4	729.1	692.9	1.0004	1.0527	?
606.0	583.8	605.7	1.0379	1.0003	CThO

<sup>a</sup> Quartet at 2024.0, 2014.0, 1970.3, 1959.8  $\text{cm}^{-1}$  in <sup>12</sup>CO + <sup>13</sup>CO. <sup>b</sup> Quartet at 2023.0, 2013.1, 1969.8, 1959.1  $\text{cm}^{-1}$  in <sup>12</sup>CO + <sup>13</sup>CO. <sup>c</sup> Triplet at 1787.6, middle band (split into 1773.6, 1772.1), 1748.0  $\text{cm}^{-1}$  in <sup>12</sup>CO + <sup>13</sup>CO. <sup>d</sup> Triplet at 1787.5, middle band (split into 1773.1, 1771.5), 1746.0  $\text{cm}^{-1}$  in C<sup>16</sup>O + C<sup>18</sup>O. <sup>e</sup> Triplet at 1724.3, 1700.9, 1687.3  $\text{cm}^{-1}$  in <sup>12</sup>CO + <sup>13</sup>CO. <sup>f</sup> Triplet at 1724.3, 1697.8, 1682.3  $\text{cm}^{-1}$  in C<sup>16</sup>O + C<sup>18</sup>O. <sup>g</sup> Triplet at 1716.7, middle band (split into 1693.5, 1691.9), 1678.9  $\text{cm}^{-1}$  in <sup>12</sup>CO + <sup>13</sup>CO. <sup>h</sup> Triplet at 1716.7, middle band (split into 1691.7, 1690.0), 1746.0  $\text{cm}^{-1}$  in C<sup>16</sup>O + C<sup>18</sup>O.

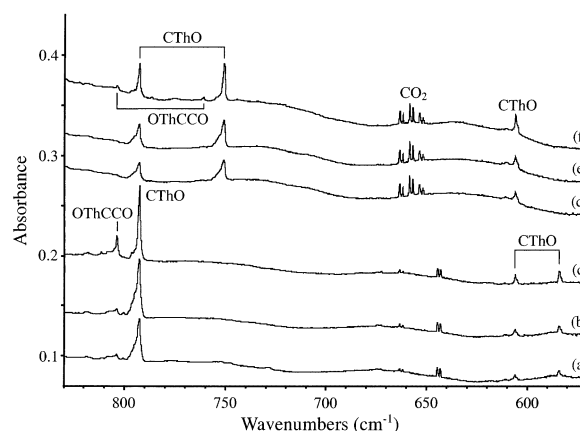


**Figure 8.** Infrared spectra in the 830–570  $\text{cm}^{-1}$  region for laser-ablated Th atoms co-deposited with isotopic CO in argon: (a) 0.2% <sup>12</sup>CO + 0.2% <sup>13</sup>CO after deposition for 70 min, (b) after  $\lambda > 470$  nm photolysis for 15 min, (c) after annealing to 25 K, (d) 0.2% C<sup>16</sup>O + 0.2% C<sup>18</sup>O after deposition for 70 min, (e)  $\lambda > 470$  nm photolysis for 15 min, and (f) after annealing to 25 K.

that it is a bent triplet molecule with calculated vibrational frequencies of 811 and 621  $\text{cm}^{-1}$ .<sup>8</sup> The 19.0 and 11.7 neon-to-argon matrix redshifts are reasonable for this molecule,<sup>36</sup> and we conclude that the same bent triplet CThO molecule is observed in solid argon as well as in solid neon. Indeed our calculations found the singlet state to be 6.6 kcal/mol higher,<sup>8a</sup> too high for matrix interactions to reverse the ground state.

The 2024.0 and 804.1  $\text{cm}^{-1}$  absorptions increase together on photolysis and annealing and are due to the OThCCO molecule,

which was observed at 2048.6 and 822.5  $\text{cm}^{-1}$  in solid neon. This molecule is predicted by DFT to be a bent singlet molecule with intense stretching modes at 2082 and 807  $\text{cm}^{-1}$ .<sup>8b</sup> With the  $^{12}\text{CO}/^{13}\text{CO}$  mixture, the upper band forms a 2024.0, 2014.0, 1970.3, 1959.8  $\text{cm}^{-1}$  quartet characteristic of a vibration involving two inequivalent carbon atoms, and with the  $\text{C}^{16}\text{O}/\text{C}^{18}\text{O}$  mixture a 2024.0, 2005.4  $\text{cm}^{-1}$  doublet indicates a single oxygen atom. The  $^{12}\text{CO}/^{13}\text{CO}$  and  $\text{C}^{16}\text{O}/\text{C}^{18}\text{O}$  ratios (1.0328 and 1.0093) are consistent with an antisymmetric C–C–O stretching mode; further, these isotopic frequency ratios are nearly the same as found for OThCCO in solid neon.<sup>8b</sup> Likewise the lower band forms a 804.1, 761.2  $\text{cm}^{-1}$  doublet for a single oxygen atom and the  $\text{C}^{16}\text{O}/\text{C}^{18}\text{O}$  ratio 1.0564 indicates a Th–O stretching mode. The 24.6 and 18.4  $\text{cm}^{-1}$  neon-to-argon matrix shifts are reasonable for OThCCO (compare 23.7 and 15.5  $\text{cm}^{-1}$  for OUCCO) and indicate that the same bent singlet OThCCO molecule is trapped in solid neon and solid argon.

A weak 748.7  $\text{cm}^{-1}$  band that results from the reaction of Th with CO was destroyed by  $\lambda > 470$  nm photolysis. This band shifted to 709.9  $\text{cm}^{-1}$  with  $\text{C}^{18}\text{O}$  ( $\text{C}^{16}\text{O}/\text{C}^{18}\text{O}$  ratio 1.0546), which is appropriate for a Th–O stretching mode. The 748.7  $\text{cm}^{-1}$  band is in very good agreement with the 761.7  $\text{cm}^{-1}$  observation of CThO<sup>−</sup> in solid neon and the computed Th–O frequency of 762  $\text{cm}^{-1}$  for the  $^2\text{A}'$  ground state.<sup>8b</sup> We conclude that CThO<sup>−</sup> is being produced in solid argon as in solid neon, with a reasonable 13.0  $\text{cm}^{-1}$  redshift upon changing from a neon to an argon matrix.

The previous neon-matrix experiments provide clear evidence for ThCO with a strong 1817.5  $\text{cm}^{-1}$  absorption. This result was corroborated by DFT calculations, which predict a 1790  $\text{cm}^{-1}$  fundamental for  $^3\Sigma^-$  ThCO.<sup>8</sup> The present argon matrix experiments reveal this band split at 1800.8, 1797.8  $\text{cm}^{-1}$  with the doublet mixed isotopic structure indicative of a single carbonyl ligand. In solid argon as in neon,<sup>8</sup>  $\lambda > 470$  nm photolysis isomerizes ThCO to CThO. Again, the 16.7–19.7  $\text{cm}^{-1}$  neon-to-argon shift is reasonable.<sup>36</sup>

The CO stretching modes of the  $\text{Th}(\text{CO})_2$  molecule were found in solid neon at 1827.7 and 1775.6  $\text{cm}^{-1}$ . Analogous bands are observed in solid argon at 1787.6 and 1716.7  $\text{cm}^{-1}$  with a 5/2 intensity ratio. As in the neon matrix, photolysis leads to disappearance of these bands and the appearance of OThCCO. Further, the isotopic structures and ratios are comparable to those observed for the bands of  $\text{Th}(\text{CO})_2$  in the neon matrix.<sup>8b</sup> We therefore assign the 1787.6 and 1716.7  $\text{cm}^{-1}$  bands to the symmetric and antisymmetric C–O stretching modes for  $\text{Th}(\text{CO})_2$  solid argon. As found in solid neon, the symmetric mode is more intense for this acute  $\text{M}(\text{CO})_2$  species.<sup>8b</sup> In this case, however, the neon-to-argon shifts of 40.1 and 58.9  $\text{cm}^{-1}$ , respectively, are larger than those observed for the other ThCO species. We have previously predicted that  $\text{Th}(\text{CO})_2$  has an unusual structure with an acute 50° C–Th–C bond angle that fosters a direct interaction between the carbon atoms. This structure leaves a large coordination vacancy on the side of the Th atom opposite the two carbonyl ligands. It may be the case that Ar atoms from the matrix are providing a nonnegligible interaction with the Th atom, causing the large matrix shifts. Indeed, our calculations indicate that the Ar atoms can bind to Th at a distance of 3.28 Å in  $\text{Ar}_n\text{Th}(\text{CO})_2$  ( $n = 2, 4$ ). When considering that the covalent radius is almost 0.2 Å larger for Th atom than for U atom, the optimized Th–Ar distance is in

fact significantly short, which is consistent with the spatially more accessible 6d orbitals in Th atom. We also note that the  $^{12}\text{CO}$ ,  $^{13}\text{CO}$  components for both bands are split about 1.5  $\text{cm}^{-1}$ , which suggests a slight inequivalence in the two carbonyl subunits. Finally, annealing the solid argon to 35–40 K produces a very strong 1980.5  $\text{cm}^{-1}$  absorption, which forms the strong 1980.5, 1936.3  $\text{cm}^{-1}$  doublet with the  $^{12}\text{CO}/^{13}\text{CO}$  mixture that is expected for  $\text{Th}(\text{CO})_6$ . The shift from the 1999.7  $\text{cm}^{-1}$  band of  $\text{Th}(\text{CO})_6$  in neon<sup>8b</sup> is appropriate for a usual matrix effect.

To examine further the matrix effects on the Th + CO chemistry, laser-ablated thorium was also reacted with 0.4% CO in krypton. The results are summarized in Table 3 and show that most of the same species are formed. As in argon, CThO was the major product observed on deposition, with slightly redshifted bands in krypton at 784.6 and 596.1  $\text{cm}^{-1}$ . Annealing to 25 and 30 K markedly increased a weak absorption at 1792.2  $\text{cm}^{-1}$ , which is assigned to ThCO. This species disappeared on full-arc photolysis, whereas the 784.6, 596.0  $\text{cm}^{-1}$  bands and weak 2020.2, 803.8  $\text{cm}^{-1}$  absorptions for OThCCO increased. Annealing to 35 and 45 K regenerated the weak 1792.2  $\text{cm}^{-1}$  band, sharpened the 784.6 and 596.0  $\text{cm}^{-1}$  bands, increased the bands at 2020.2 and 803.8  $\text{cm}^{-1}$ , and produced a strong 1976.7  $\text{cm}^{-1}$  absorption for  $\text{Th}(\text{CO})_6$ . An experiment with 0.4%  $^{12}\text{CO}$  + 0.4%  $^{13}\text{CO}$  in krypton gave the major CThO product at 784.6  $\text{cm}^{-1}$  with a weak doublet at 596.1–574.3  $\text{cm}^{-1}$ . The  $^{12}\text{CO}/^{13}\text{CO}$  ratio, 1.0380, is unchanged from the argon matrix ratio. A ThCO doublet at 1792.2–1753.0  $\text{cm}^{-1}$  increased on 25 K annealing and decreased on  $\lambda > 470$  nm photolysis. A sharp OThCCO quartet observed at 2020.2, 2009.5, 1967.0, 1955.4  $\text{cm}^{-1}$  increased on  $\lambda > 470$  nm photolysis along with an 803.8  $\text{cm}^{-1}$  band. New 2/1 relative intensity bands observed at 1780.3 and 1704.1  $\text{cm}^{-1}$  decrease slightly on  $\lambda > 470$  nm photolysis, shift to 1741.0 and 1666.8  $\text{cm}^{-1}$  with  $^{13}\text{CO}$ , and show new 1765.9 and 1681.2  $\text{cm}^{-1}$  intermediate components with  $^{12}\text{CO}$  +  $^{13}\text{CO}$ . These bands are appropriate for  $\text{Th}(\text{CO})_2$  in solid krypton. Final annealing produced a very strong broad 1976.7–1934.5  $\text{cm}^{-1}$  doublet for  $\text{Th}(\text{CO})_6$ .

## Discussion

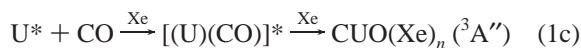
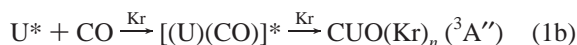
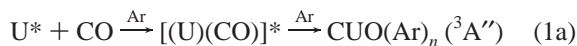
### Reactions and Products in Different Noble-Gas Matrices.

The experimental observations reported here and earlier<sup>5,11,12</sup> indicate that laser-ablated U atoms with excess energy or photoexcited U atoms react with CO in noble-gas carriers to form CUO, which is trapped in the solid noble-gas matrix. In excess argon, krypton, or xenon, CUO is trapped in a triplet state in the matrix (eq 1). These results contrast those in solid neon, in which CUO is trapped as a singlet molecule, although doping of neon with 1% Ar is sufficient to trap CUO in its triplet state.<sup>12</sup> The insertion of a metal atom into the robust triple bond of CO is unique and has only been observed for the actinides U and Th<sup>5,8</sup> and for niobium upon photoisomerization of NbCO.<sup>39</sup> In argon and krypton the CUO molecule captures an electron to form the same bent doublet CUO<sup>−</sup> anion that was observed in solid neon (eq 2). Our relativistic DFT calculations find eq 2 to be exothermic by 24 kcal/mol, so  $\lambda > 470$  nm radiation is more than capable of causing electron photodetachment. CUO in argon and krypton matrices also reacts with CO to produce the linear triplet OUCCO molecule,

(39) Zhou, M. F.; Andrews, L. *J. Phys. Chem. A* **1999**, *103*, 7785 (Nb, Ta + CO).



a reaction also observed in solid neon (eq 3). We calculate that this reaction is exothermic by 69 kcal/mol



The major physical differences of interest here among the series of noble gases are their polarizabilities and freezing points, which determine the inertness and rigidity of the solids formed as matrix hosts. The initial product yield is higher in neon because of increased reagent diffusion and reaction during the slower condensation of neon at 4 K than of argon and krypton at 7 K. In contrast, more diffusion can take place in annealed argon and krypton due to the wider temperature range of the solid and the greater interatomic separations in the solid. Hence, the formation of  $\text{U}(\text{CO})_6$  is greatly enhanced on annealing in solid argon ( $1961.3 \text{ cm}^{-1}$ ), in agreement with previous workers,<sup>38</sup> and in solid krypton ( $1964.5 \text{ cm}^{-1}$ ) relative to the results in solid neon.

The matrix photochemistry is slightly different in the different noble-gas matrices. The yield of the UV photolysis products OUCCO and  $(\text{C}_2)\text{UO}_2$  is higher in solid neon because the neon matrix is more UV transparent, but OUCCO is clearly formed in solid argon and krypton as well from the isomerism of  $\text{U}(\text{CO})_2$ . No  $(\text{C}_2)\text{UO}_2$  was produced in solid krypton. The  $\text{CUO}^-$  anion is photodetached by  $\lambda > 470 \text{ nm}$  radiation in solid argon whereas  $\lambda > 380 \text{ nm}$  photolysis was required in solid neon.

The different noble gases lead to small differences in the vibrational frequencies for OUCCO ( $2051.5, 1361.8, 841.0 \text{ cm}^{-1}$  in neon;  $2027.8, 1352.8, 825.5 \text{ cm}^{-1}$  in argon;  $2021.4, 826.7 \text{ cm}^{-1}$  in krypton),  $\text{CUO}^-$  ( $929.3, 803.3 \text{ cm}^{-1}$  in neon;  $924.2, 798.1 \text{ cm}^{-1}$  in argon) and  $(\text{C}_2)\text{UO}_2$  ( $922.1 \text{ cm}^{-1}$  in neon;  $908.5 \text{ cm}^{-1}$  in argon). These are all typical matrix shifts that can be ascribed to the different polarizabilities of the matrix atoms.<sup>36</sup> Furthermore, the isotopic frequency ratios are essentially unchanged so the normal modes are not altered by the matrix cage. The results for CUO are in marked contrast to those for the other molecules; however, the frequencies observed in solid argon ( $852.5, 804.3 \text{ cm}^{-1}$ ) and krypton ( $842.3, 797.1 \text{ cm}^{-1}$ ) are very similar but differ substantially from those observed in solid neon ( $1047.3, 872.2 \text{ cm}^{-1}$ ). In addition, the isotopic frequency ratios in argon and krypton are markedly different from those in neon, indicating different normal modes and hence different electronic states of CUO as discussed above, are trapped in neon and the heavier noble gas solids. Our DFT calculations on the isolated CUO molecule find a triplet state about 1 kcal/mol above the singlet ground state,<sup>5</sup> but we have also pointed out that complexation of CUO with noble-gas atoms preferentially lowers the triplet state more than the singlet state.<sup>12</sup> We will discuss this effect in greater detail below. It is noteworthy that

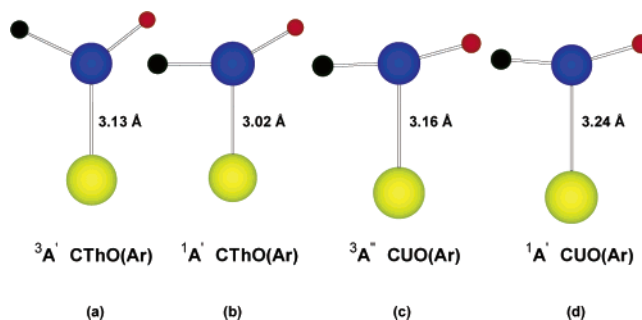


**Figure 9.** Structures of singlet and triplet CThO(Ar) and CUO(Ar) calculated by relativistic DFT (atoms: black C, blue Th, U, red O, yellow Ar).

evidence has also been presented for  $\text{UO}_2$  and for FeCO trapped in different electronic states in solid neon and argon.<sup>2,40</sup>

Electronic transitions are typically red-shifted in solid argon relative to solid neon owing to a stronger interaction between the excited-state molecule and the matrix. For example, the near-ultraviolet transitions for TaO are red-shifted  $200\text{--}300 \text{ cm}^{-1}$  from neon to argon.<sup>41</sup> In the present case, it would be intriguing to observe the  $\text{T} \leftarrow \text{S}$  electronic transition of CUO in solid neon or the  $\text{S} \leftarrow \text{T}$  electronic transition of  $\text{CUO}(\text{Ar})_n$  in argon. Unfortunately, these electronic transitions, which have  $\Phi$  symmetry in the  $\text{C}_{\infty v}$  single-group and  $\Phi + \Delta + \Gamma$  symmetries in the  $\text{C}_{\infty v}$  double-group, are not electric-dipole allowed. As a result, no such bands were found in the  $4000\text{--}450 \text{ cm}^{-1}$  range.

In contrast to the results for CUO, all of the thorium-containing species observed here exhibit typical matrix shifts from neon to argon to krypton with virtually unchanged isotopic frequency ratios. These results indicate that the same electronic state of each species is trapped in the three matrices. In the case of isolated CThO, we calculate that the lowest singlet state is  $6.6 \text{ kcal/mol}$  higher in energy than the  ${}^3\text{A}'$  ground state,<sup>8a</sup> and the bent triplet is apparently the ground state in solid neon, argon, and krypton. Indeed, when an Ar atom is included in the calculation, the corresponding triplet of CThO(Ar) is still  $3.8 \text{ kcal/mol}$  more stable than its singlet counterpart; Ar–Th bonding is not sufficient to alter the ground state of CThO. Interestingly, the CThO(Ar) molecule possesses shorter Th–Ar distances ( $3.13$  and  $3.02 \text{ \AA}$ ) and larger CThO–Ar binding energies ( $4.7$  and  $7.6 \text{ kcal/mol}$  for the triplet and singlet) than the CUO(Ar) counterparts, consistent with the more diffuse  $6d$  orbitals in Th than in U. The structures of the  ${}^3\text{A}'$  and  ${}^1\text{A}'$  states of CThO(Ar) are shown in Figure 9a,b.

**Structure and Bonding of  $\text{CUO}(\text{Ng})_n$  ( $n > 1$ ) Complexes.** The energetic closeness of the singlet and triplet states of CUO, and the fact that the presence of Ar, Kr, or Xe atoms is sufficient to reduce and eventually reverse the relative energies between these states, are the electronic effects that allowed us to uncover the remarkable interactions between the CUO molecule and noble-gas atoms via vibrational spectroscopy. To understand better the state energetics and the interactions between noble-gas atoms and the CUO molecule, we have performed relativistic DFT calculations using very diffuse basis sets to improve the performance for noble-gas systems.<sup>42,43</sup>

We have previously suggested that the interaction of CUO with a single Ar atom will stabilize triplet CUO(Ar) more than

(40) Zhou, M.; Andrews, L. *J. Chem. Phys.* **1999**, *110*, 10370 (Fe + CO).

(41) Weltner, W., Jr.; McLeod, D., Jr. *J. Chem. Phys.* **1965**, *42*, 882 (Table 5).

(42) Frenking, G.; Cremer, D. *Struct. Bonding (Berlin)* **1990**, *73* 17.

for the singlet form of the molecule.<sup>12</sup> The experimental results presented here provide indisputable evidence for the binding of multiple noble-gas atoms to the CUO molecule, making it unlikely that isolated “mono-noble-gas” CUO(Ng) species exist in the heavier noble gas solids. Nevertheless, the results we obtain on the series of CUO(Ng) molecules are instructive inasmuch as they show the formation of U–Ng bonds and the change in the ground-state multiplicity upon this bonding. We will therefore begin with a discussion of the bonding in CUO(Ng) model complexes, and will follow that with a description of the bonding in the CUO(Ng)<sub>n</sub> complexes.

Calculations on CUO(Ar) were carried out with the CUO molecule in its <sup>1</sup>Σ<sup>+</sup> (<sup>1</sup>A′) ground state and its low-lying <sup>3</sup>Φ (<sup>3</sup>A′′) excited state, where the Greek state designations are for the linear (C<sub>∞v</sub> symmetry) geometry of CUO whereas the designations in parentheses are appropriate for C<sub>s</sub> symmetry. We find that CUO(Ar) is a planar molecule with a <sup>3</sup>A′′ ground state and a bent CUO fragment (∠CUO = 166.5°) bound to the Ar atom primarily through the U atom (Figure 9c). At the DFT level in the absence of spin–orbit coupling, the <sup>3</sup>A′′ state of CUO(Ar) is calculated to be slightly lower than the <sup>1</sup>A′ state. The U–Ar distance in the converged triplet structure is 3.16 Å, which is smaller than the sum of the crystal radii of the two elements (3.25 Å),<sup>44</sup> but much longer than the 2.49 Å length<sup>45</sup> of the U–Cl chemical bond in UCl<sub>6</sub>. Thus, we indeed have an equatorial complex, rather than a chemical bond.

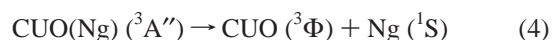
For both isolated CUO and CUO(Ar), the triplet state corresponds to the transfer of an electron from an orbital that has significant U–C σ bonding character to a nonbonding U 5f orbital. As a consequence, the U–C bond is longer and weaker in the triplet states of CUO and CUO(Ar) than in the singlet state. The U–C bond is nearly 0.1 Å longer in triplet CUO (U–C = 1.846 Å) than in singlet CUO (U–C = 1.747 Å). The U–C bonds in both states of CUO(Ar) are slightly longer than those in the corresponding state of CUO and show the same magnitude of lengthening from singlet to triplet (U–C in singlet CUO(Ar) = 1.752 Å; U–C in triplet CUO(Ar) = 1.858 Å). For both CUO and CUO(Ar), the U–O bond length is only slightly affected by the change from singlet to triplet. In CUO, for example, the calculated U–O bond length is 1.804 Å in the singlet state and 1.818 Å in the triplet state.

The fact that the singlet and triplet states of CUO are so close in energy is a consequence of a delicate balance between opposing effects, much as is the case for high- and low-spin transition metal complexes. In the closed-shell singlet state, the U–C bonding is significantly stronger than in the triplet state, wherein one of the U–C bonding electrons has been transferred to a nonbonding U 5f orbital. This effect is countered by increased exchange stabilization and decreased Coulomb repulsion in the open-shell triplet state. In isolated CUO, the increased strength of the U–C bonding dominates, and the singlet state is the ground state. When Ar atoms are present, however, the interaction of the Ar atoms with the CUO molecule stabilizes

the triplet state more than the singlet state, which causes the triplet state of CUO(Ar) to be energetically close to the singlet state.

There are two primary reasons that the triplet state of CUO interacts more strongly with an Ar atom than does the singlet state, both of which arise because the primary mode of the interaction of the Ar atom with CUO is donation from a filled orbital of Ar atom into an empty primarily 6d orbital localized on the U atom. First, because the U–C distance is longer in triplet CUO, the Ar atom experiences less repulsion from the U and C atoms in the triplet state than in the singlet state. As a consequence, the Ar atom is able to approach the U atom more closely, as is clear from the U–Ar distances in the converged structures of triplet (U–Ar = 3.16 Å) and singlet (U–Ar = 3.24 Å CUO(Ar) (Figure 9c,d). Indeed, geometry optimizations of the CUO(Ar) complex indicate that the U–Ar distance decreases further by 0.05 Å when the second electron is transferred from the U–C σ-bonding orbital to the U 5f orbitals. Second, the transfer of an electron from a U–C bonding orbital to a U 5f orbital affects a partial reduction of the U atom. The expansion of the U 6d orbitals upon this reduction leads to greater overlap and a stronger interaction between the U and Ar atoms. Thus, the U–Ar bond is essentially the result of a Lewis acid–base interaction that is facilitated by the longer U–C bond and the more diffuse U atom in the triplet state. It is remarkable that this weak interaction is sufficient to reverse the energies of the triplet and singlet states when enough Ar atoms are bonded.

The fact that the bond between U and Ar in CUO(Ar) is a Lewis acid–base interaction led us to predict that the bonding would be even stronger for heavier, more polarizable noble gases. Indeed, our calculations on CUO(Kr) and CUO(Xe) find that the U–Ng bond strength increases steadily from Ar to Kr to Xe, as gauged by the calculated dissociation energy for the following reaction



We find that the calculated dissociation energies of CUO(Ng) (<sup>3</sup>A′′) for eq 4 are 3.7, 4.9, and 7.3 kcal/mol for Ar, Kr, and Xe, respectively, corresponding to CUO(<sup>1</sup>Σ<sup>+</sup>)-Ng(<sup>1</sup>S) binding energies of 3.2, 4.4, and 6.8 kcal/mol. We also find that the stronger U–Ng interactions for Kr and Xe lead to greater stabilization of the triplet state of CUO(Ng) relative to the singlet state.

**Structure and Bonding of CUO(Ng)<sub>4</sub> Complexes.** In matrices with 1–2% Kr in argon, 1–3% Xe in argon, and 2% Xe in krypton the bands due to CUO are split into new four-band progressions suggesting that at least four Ng atoms can complex to CUO depending on the experimental conditions. The involvement of multiple noble-gas atoms has precedent in other systems: Xenon atoms appear to solvate HXeBr and HXeCl in neon matrices even with small amounts of Xe depending on concentration and annealing history.<sup>46</sup> To explore further the bonding of multiple noble-gas atoms to CUO, we calculated structures of CUO(Ng)<sub>n</sub> (Ng = Ar, Kr, Xe; n = 2–6) complexes. Figure 10 presents plots of the total Ng binding energy as a function of n for the triplet CUO(Ng)<sub>n</sub> complexes,

(43) Lundell, J.; Chaban, G. M.; Gerber, R. B. *J. Phys. Chem. A* **2000**, *104*, 7944.

(44) Our preliminary calculations using the much more accurate coupled-cluster CCSD(T) method predict similar U–Ar distances of 3.30 and 3.21 Å for the singlet and triplet states, respectively. For the radii, see Winter, M. J. WebElements [http://www.webelements.com/] (WebElements Ltd., Sheffield, UK, 2001).

(45) Schreckenbach, G. *Inorg. Chem.* **2000**, *39*, 1265.

(46) Lorenz, M.; Räsänen, M.; Bondybey, V. E. *J. Phys. Chem. A* **2000**, *104*, 3770.

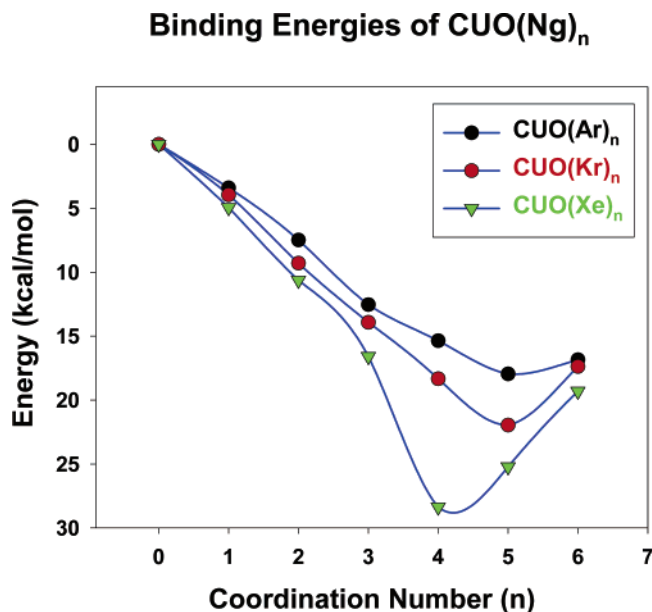


**Figure 10.** Binding energies for  $\text{CUO}(\text{Ar})_n$ ,  $\text{CUO}(\text{Kr})_n$ , and  $\text{CUO}(\text{Xe})_n$  in triplet states.

which were calculated as the energy change for the following process



For the  $\text{CUO}(\text{Ar})_n$  complexes, the magnitude of the total binding energy increases monotonically through  $n = 5$ . When  $n = 6$ , however, the magnitude of the binding energy decreases, indicating an overall repulsion for binding the sixth Ar atom. Thus, these results suggest that, in the gas phase,  $\text{CUO}(\text{Ar})_5$  represents the optimum coordination of Ar atoms around the CUO molecule. However, although we predict that five Ar atoms can bind to CUO in the gas phase, we believe that the octahedral symmetry expected in the face-centered-cubic solid argon lattice and the effect of solvation by the next layer of argon atoms could favor  $\text{CUO}(\text{Ar})_4$  in pure solid argon. At present, we do not have experimental evidence to determine whether CUO in solid argon exists preferentially as  $\text{CUO}(\text{Ar})_4$  or  $\text{CUO}(\text{Ar})_5$ , so we will denote the CUO in pure argon as  $\text{CUO}(\text{Ar})_n$  where  $n = 4$  or  $5$ .

For the larger noble gas atoms Kr and Xe, our calculations indicate that the optimum structures are  $\text{CUO}(\text{Kr})_5$  and  $\text{CUO}(\text{Xe})_4$ , respectively. The prediction of five-coordination of Kr is curious and is not supported by the experimental data or by a simple geometric model where the Ng atoms are separated by more than twice their van der Waals radii when at typical U–Ng bond lengths. Thus, five Ar atoms in a regular pentagonal arrangement saturate the equatorial plane around CUO; when the Ar atoms are separated by twice the van der Waals radius ( $3.76 \text{ \AA}$ ),<sup>44</sup> the U–Ar distance is  $3.20 \text{ \AA}$ , which is very near the optimized U–Ar distances computed here. The same simple model predicts that no more than four Kr or Xe atoms can surround the CUO molecule, which is consistent with the DFT binding-energy calculations for Xe but not for Kr. Because our calculations with diffuse functions on the energy of  $\text{CUO}(\text{Kr})_5$  have large error due to poor fitting of the Coulomb potentials, it is possible that the DFT result predicting  $\text{CUO}(\text{Kr})_5$  is incorrect, and that a maximum of four Kr or Xe atoms occupy

the primary coordination sphere of CUO. In support of this notion, preliminary calculations on the total binding energies of  $\text{CUO}(\text{Kr})(\text{Ar})_n$  and  $\text{CUO}(\text{Xe})(\text{Ar})_n$  indicate that  $n = 3$  is the optimum value, i.e., when a single Kr or Xe atom is coordinated to CUO, the U atom prefers a six-coordinate octahedral arrangement of bonded atoms. The experiments using matrixes of dilute Kr in Ar or dilute Xe in Ar suggest the sequential complexation of one, two, three, or four Kr or Xe atoms, where the Kr or Xe atoms apparently displace Ar atoms. We therefore propose that the progressions in Figures 4 and 5 are due to the sequential formation of the six-coordinate complexes  $\text{CUO}(\text{Ar})_{4-n}(\text{Kr})_n$  and  $\text{CUO}(\text{Ar})_{4-n}(\text{Xe})_n$  ( $n = 1, 2, 3, 4$ ) upon annealing of the matrix. The experimental data suggest that the U–C and U–O stretching frequencies are perturbed more by the replacement of Ar with Xe than by Kr. The U–C and U–O frequencies decrease by roughly  $1.6$  and  $1.2 \text{ cm}^{-1}$ , respectively, upon replacement of Ar by Kr, and by  $4$  and  $3 \text{ cm}^{-1}$ , respectively, upon replacement of Ar by Xe (Table 4).

Table 6 presents the calculated binding energies, geometries, and vibrational frequencies of the  $\text{CUO}(\text{Ar})_{4-n}(\text{Xe})_n$  ( $n = 1, 2, 3, 4$ ) complexes. Results for  $\text{CUO}(\text{Ar})_{4,5}$  and  $\text{CUO}(\text{Kr})_4$  are included for completeness. Several aspects of the calculated properties provide strong support for the notion of successive substitution of Ar by Xe in these complexes. First, the complexes are all predicted to have a triplet ground state (ignoring spin–orbit effects) and therefore the vibrational frequencies are distinctly different than for CUO in solid Ne, which has a singlet ground state.<sup>5,11,12</sup> Second, with one exception, the total binding energy increases monotonically with increasing Xe substitution. The calculations on  $\text{CUO}(\text{Ar})_2(\text{Xe})_2$  were not well-behaved with this basis set, once again due to poor fitting in the Coulomb potentials, and we suspect that the calculated binding energy of  $26.6 \text{ kcal/mol}$  for *trans*- $\text{CUO}(\text{Ar})_2(\text{Xe})_2$  is somewhat too high. Finally, the calculated frequencies of the  $\text{CUO}(\text{Ar})_{4-n}(\text{Xe})_n$  series exhibit the monotonic red-shift upon successive replacement of Ar atoms by Xe atoms. The calculated red-shifts are somewhat smaller than those observed experimentally: The calculated U–C and U–O stretching frequencies shift  $11$  and  $5 \text{ cm}^{-1}$  lower from  $\text{CUO}(\text{Ar})_4$  to  $\text{CUO}(\text{Xe})_4$  vs experimental shifts of  $17$  and  $12 \text{ cm}^{-1}$  from  $\text{CUO}(\text{Ar})_n$  to  $\text{CUO}(\text{Xe})_4$ . The calculated U–C and U–O frequencies are roughly  $30$  to  $35$  and  $20$  to  $25 \text{ cm}^{-1}$  higher than those observed experimentally, respectively, which may be due in part to solvation effects of the argon matrix and the omission of spin–orbit coupling effects. Nevertheless, the calculated frequencies and predicted red-shifts are in satisfyingly good accord with the experimental observations.

The significance of second-shell solvation effects may be indicated by small changes in the CUO frequencies of analogous complexes when the host matrix is changed. For example,  $\text{CUO}(\text{Xe})_4$  in argon red-shifts  $3.2$  and  $2.1 \text{ cm}^{-1}$  in krypton and  $5.6$  and  $3.4 \text{ cm}^{-1}$  in pure xenon. In addition, the  $\text{CUO}(\text{Kr})_4$  complex in argon red shifts  $3.7$  and  $2.3$  when pure krypton is used. Figure 7 shows the small secondary matrix solvent shifts for  $\text{CUO}(\text{Xe})_4$  in the argon matrix as compared to krypton.

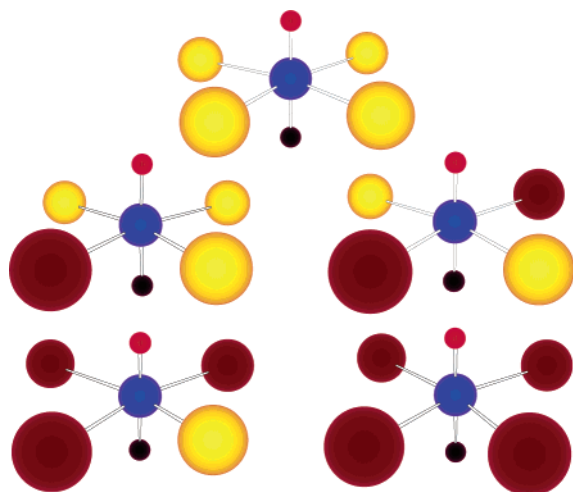
The experimental observations combined with relativistic DFT calculations provide strong evidence that the bands at  $848.0$ ,  $843.6$ ,  $839.4$ , and  $835.4 \text{ cm}^{-1}$  are due to  $\text{CUO}(\text{Ar})_3(\text{Xe})$ ,  $\text{CUO}(\text{Ar})_2(\text{Xe})_2$ ,  $\text{CUO}(\text{Ar})(\text{Xe})_3$ , and  $\text{CUO}(\text{Xe})_4$ , respectively. Figure 11 illustrates the calculated structures of these com-



**Table 6.** Optimized Geometries, Binding Energies, and Calculated Stretching Frequencies of  $\text{CUO}(\text{Ar})_{4-n}(\text{Xe})_n$  ( $n = 0, 1, 2, 3, 4$ ) Complexes<sup>a</sup>

	state	$E_{\text{bind}}$	U–C	U–O	U–Ar	U–Xe(Kr)	$\nu(\text{U–C})$	$\nu(\text{U–O})$
$\text{CUO}(\text{Ar})_4$	$^3\text{B}_2$	15.4	1.868	1.843	$3.185 \times 4$	-	881	824
$\text{CUO}(\text{Kr})_4$	$^3\text{B}_2$	18.3	1.873	1.839	-	$3.258 \times 4$	876	822
$\text{CUO}(\text{Ar})_3(\text{Xe})$	$^3\text{A}''$	17.7	1.872	1.842	$3.214 \times 2$ 3.228	3.360	877	824
$\text{CUO}(\text{Ar})_2(\text{Xe})_2$ <sup>b</sup>	$^3\text{B}_2$	26.6	1.882	1.846	$3.118 \times 2$	$3.379 \times 2$	875	823
$\text{CUO}(\text{Ar})(\text{Xe})_3$	$^3\text{A}''$	23.2	1.877	1.838	3.145	$3.358 \times 2$ 3.574	873	820
$\text{CUO}(\text{Xe})_4$	$^3\text{B}_2$	28.4	1.875	1.833	-	$3.369 \times 4$	870	819
$\text{CUO}(\text{Ar})_5$	$^3\text{A}''$	17.9	1.868	1.841	3.22–3.26	-	880	822

<sup>a</sup> The binding energies are in kcal/mol, the bond lengths in Å, and the frequencies in  $\text{cm}^{-1}$ . All quantities are calculated using the Vdiff basis sets with 2f diffuse functions deleted. <sup>b</sup> Only the trans isomer of  $\text{CUO}(\text{Ar})_2(\text{Xe})_2$  converged with this basis set.

**Figure 11.** Structures for  $\text{CUO}(\text{Ar})_{4-n}(\text{Xe})_n$ ,  $n = 0, 1, 2, 3, 4$ .

plexes, along with that of  $\text{CUO}(\text{Ar})_4$  for comparison. We calculate the total  $\text{CUO–Xe}$  binding energy in  $\text{CUO}(\text{Xe})_4$  as a substantial 28.4 kcal/mol, leading to an average  $\text{U–Xe}$  bond energy of 7.1 kcal/mol. The observations for  $\text{CUO}$  with dilute Kr in solid argon give parallel results, with the formation of the Kr complexes  $\text{CUO}(\text{Ar})_{4-n}(\text{Kr})_n$  ( $n = 1, 2, 3, 4$ ). Likewise  $\text{CUO}$  in the presence of Xe in krypton gives analogous  $\text{CUO}(\text{Kr})_{4-n}(\text{Xe})_n$  complexes. As expected, the red-shifts of the stretching frequencies induced upon substitution of Ar with Kr and Kr with Xe are smaller than those upon substitution of Ar with Xe, but the sum of the former two is almost equal to the latter red-shifts (peak separations in four-band progressions).

As noted earlier, both the experiments and the calculations indicate a small red-shift of the  $\text{CUO}$  modes upon substitution of a lighter noble-gas atom with a heavier one. We also note slight changes in the isotopic frequency ratios for the 848.0 and 801.3  $\text{cm}^{-1}$  bands of  $\text{CUO}(\text{Ar})_3(\text{Xe})$  in solid argon relative to those of  $\text{CUO}(\text{Ar})_n$  (Table 2). For the lower-energy band, the  $^{12}\text{C}/^{13}\text{C}$  and  $\text{C}^{16}\text{O}/\text{C}^{18}\text{O}$  ratios for  $\text{CUO}(\text{Ar})_3(\text{Xe})$  respectively increase and decrease slightly relative to  $\text{CUO}(\text{Ar})_n$ . The behavior of the isotopic ratios for the higher-energy band is opposite that of the lower band: the  $^{12}\text{C}/^{13}\text{C}$  and  $\text{C}^{16}\text{O}/\text{C}^{18}\text{O}$  ratios decrease and increase, respectively. Thus, for each of the bands, the larger ratio decreases slightly and the smaller ratio increases slightly upon substitution, implying that substitution by Xe induces greater mode mixing between the “pure”  $\text{U–C}$  and  $\text{U–O}$  stretching modes. A similar trend is found for the  $\text{CUO}(\text{Kr})$  species in solid argon. Both of these trends have been confirmed by the calculated DFT normal modes.

A closer examination of the electronic structure of  $\text{CUO}(\text{Ng})_4$  reveals the nature of the  $\text{U–Ng}$  bonding in these new octahedral complexes. We will discuss the bonding in  $\text{CUO}(\text{Ar})_4$  to show the major interactions that occur, and use those results to explain the changes that occur upon substitution of Ar by a heavier Kr or Xe atom. The  $\text{U–Ar}$  interactions in  $\text{CUO}(\text{Ar})_4$  are similar to those discussed earlier for  $\text{CUO}(\text{Ar})$ , although the higher symmetry of the larger complex makes the discussion somewhat clearer. Our calculations predict that ground-state  $\text{CUO}(\text{Ar})_4$  is a triplet  $C_{4v}$  molecule with a linear  $\text{CUO}$  fragment and essentially octahedral coordination about the U atom (Figure 11). The Ar atoms are slightly displaced toward the C atom ( $\angle\text{C–U–Ar} = 84.6^\circ$ ), much as the Ar atom in  $\text{CUO}(\text{Ar})$  is closer to the C atom than to the O atom (Figure 9).

The weak interactions between the Ar atoms and the U atom of  $\text{CUO}$  involve  $\sigma$ -donation from an Ar lone pair into empty primarily U-based orbitals. Although in principle Ar could act as a  $\pi$  donor toward the U atom as well, we see no evidence for any significant  $\text{Ar–U}$   $\pi$  donation. Under  $C_{4v}$  symmetry, the Ar  $\sigma$ -donor lone pairs lead to symmetry-adapted linear combinations of  $a_1$ ,  $b_2$ , and  $e$  symmetry (in our coordinate system, the Ar atoms lie along the lines  $y = \pm x$ ). These Ar group orbitals can, in principle, interact with the vacant U 7s orbital ( $a_1$ ), U 7p orbitals ( $a_1 + e$ ), U 6d orbitals ( $a_1 + b_2 + e$ ), or U 5f orbitals ( $a_1 + b_2 + e$ ). In general, ligand donation to actinide atoms preferentially involves the U 6d orbitals.<sup>47</sup> Indeed, we find that the most significant Ar-to-U donation occurs in a bonding molecular orbital of  $b_2$  symmetry that involves donation from the filled Ar 3p orbitals into the empty 6d<sub>xy</sub> orbital. This MO is composed of roughly 96% Ar 3p and 4% U 6d character. It is therefore best described as a weak Lewis acid–base interaction between the Ar 3p (Lewis base) and U 6d (Lewis acid) orbitals. Some other MOs of triplet  $\text{CUO}(\text{Ar})_4$  involve 1–2% uranium-based orbitals, and represent additional Ar-to-U donation. As is pointed out in uranyl bonding, the semi-core 6p orbitals can have bonding interaction with the Ar 2s and 2p orbitals, which gives rise to the so-called “U 6p core hole”.<sup>48</sup>

Mulliken population analysis<sup>49</sup> of the converged electronic structures can provide an indication of the changes that occur when four Ar atoms bond to  $\text{CUO}$ . However, the very diffuse basis functions that are used in these calculations cause a well-known breakdown of the Mulliken population model, which assumes that basis functions maximize closest to the atom on which they are centered. To examine meaningful Mulliken

(47) Pepper, M.; Bursten, B. E. *Chem. Rev.* **1991**, *91*, 719.(48) Larsson, S.; Pyykkö, P. *Chem. Phys.* **1986**, *101*, 355.(49) Mulliken, R. S. *J. Chem. Phys.* **1955**, *23*, 1833.

populations, we have performed additional calculations at the converged geometry using a reduced basis set in which the diffuse functions have been removed. Using this reduced basis, the Mulliken charge on the U atom in  $^3\Phi$  CUO is +1.43. Binding four Ar atoms to form  $^3B_2$  CUO(Ar) $_4$  reduces the Mulliken charge on U to +1.31. Consistent with the discussion above, the largest change in the U Mulliken populations occurs in the 6d orbitals. The total 6d orbital population in triplet CUO is 1.73, whereas in triplet CUO(Ar) $_4$  it is 1.83, which accounts for 83% of the charge reduction. The Mulliken charge on the four Ar atoms in triplet CUO(Ar) $_4$  is +0.16, an indication that each Ar atom is donating about 0.04 of an electron to the CUO molecule.

As noted above, triplet CUO(Ar) $_4$  is about 4.5 kcal/mol below the singlet form of the molecule. The reasons that the triplet form of the molecule is favored are entirely analogous to our discussion above about CUO(Ar). The calculated U–C bond length in triplet CUO(Ar) $_4$  (1.868 Å) is more than 0.1 Å longer than that in the singlet form of the molecule (1.757 Å), thus allowing a closer approach of the Ar atoms: We calculate that the U–Ar bond length in triplet CUO(Ar) $_4$  (3.185 Å) is more than 0.1 Å shorter than that in the singlet molecule (3.289 Å). Also, as in CUO(Ar), the expansion of the U 6d orbitals upon reduction of U facilitates stronger Ar-to-U donation. The Lewis acid–base description of U–Ng bonding leads to the prediction that heavier, more polarizable noble-gas atoms should bind more strongly to CUO than do lighter ones. That notion is consistent with both our experimental and computational results. In fact, the calculated U–Xe interaction is an order-of-magnitude larger than the van der Waals interaction in Xe $_2$  (0.56 kcal/mol).<sup>50</sup> We have seen that Kr and Xe atoms readily replace Ar in the coordination sphere about CUO, and Xe will replace Kr. The calculated binding energies for the CUO(Ng) $_4$  species are consistent with these observations: The binding energies per Ng atom are 3.9, 4.6, and 7.1 kcal/mol for CUO(Ar) $_4$ , CUO(Kr) $_4$ , and CUO(Xe) $_4$ , respectively. Thus, it appears that the substitution chemistry of noble gases on CUO is largely driven by enthalpic factors related to the strengths of the U–Ng bonds.

The observation that the U–C and U–O stretching frequencies slightly red-shift on substitution of a lighter noble-gas atom with a heavier one is largely tied to electronic structure as well, rather than the mass effects of the heavier noble-gas atoms. The heavier noble-gas atoms are slightly better electron donors to CUO than are Ar atoms and thus make the uranium atom slightly more electron rich. Indeed, in CUO(Xe) $_4$  the four Xe atoms donate 0.21e, whereas the U charge is 0.08e more comparing to that in CUO(Ar) $_4$ . Although the U–C and U–O bonds have large covalent components, they also depend on significant donation from the formal C $^{4-}$  and O $^{2-}$  to the U atom. When Kr or Xe atoms are bonded to CUO, the donation from C and O is slightly suppressed, leading to slightly weaker U–C and U–O bonds and the resultant red-shift. This inductive influence of the noble-gas atoms on the U–C and U–O stretching frequencies is largely driven by the number of each type of noble-gas atom bonded to CUO, and is not expected to be significantly affected by stereochemistry. We are therefore not surprised that we do not find experimental evidence for both the cis and trans isomers of CUO(Ar) $_2$ (Xe) $_2$ .

The new CUO(Ar) $_{4-n}$ (Ng) $_n$  complexes reported here are the only known examples of neutral metal complexes involving four noble gas atoms. Of these new complexes, CUO(Xe) $_4$  exhibits the strongest U–Xe bonding, and it is thus interesting to compare the properties of CUO(Xe) $_4$  with those of other metal–Xe compounds. The calculated U–Xe distance of 3.37 Å in CUO(Xe) $_4$  is, of course, significantly longer than the experimental Au–Xe distance of 2.74 Å in AuXe $_4^{2+}$ ;<sup>51</sup> the Au–Xe bonding in this dicationic complex (as well as that in AuXe $^+$  and AuXe $_2^+$ ) is strongly enhanced by the charge-induced dipole interactions involving the Au $^{2+}$  cation.<sup>52,53</sup> We must compare CUO(Xe) $_4$  with the experimentally observed neutral transition metal complexes XeM(CO) $_5$  (M = Cr, Mo, W). The calculated M–Xe distances in these carbonyl complexes, 2.99 Å (Cr), 3.10 Å (Mo), and 3.06 Å (W),<sup>15</sup> are comparable to the U–Xe distances predicted here, especially when the larger size of U is considered. The measured M–Xe dissociation energies in the XeM(CO) $_5$  complexes, 9.0 (Cr), 8.0 (Mo), and 8.2 (W) kcal/mol,<sup>13,14</sup> are comparable with those computed here for U–Xe.

The present spectra clearly show that four Ng atoms are involved in the intimate coordination sphere around uranium. This work provides conclusive evidence for distinct CUO(Ar) $_{4-n}$ (Ng) $_n$  (Ng = Kr, Xe;  $n = 1, 2, 3, 4$ ) and CUO(Kr) $_{4-n}$ (Xe) $_n$  complexes, and the first characterization of neutral complexes involving four noble-gas atoms on one metal center.

## Conclusions

Laser-ablated U atoms react with CO in excess argon to produce CUO, which is trapped as a triplet-state complex in solid argon at 7 K, based on agreement between observed and relativistic density functional theory calculated isotopic frequencies ( $^{12}C^{16}O$ ,  $^{13}C^{16}O$ ,  $^{12}C^{18}O$ ). This contrasts the neon matrix environment, which trapped CUO in a linear singlet state calculated to be about 1 kcal/mol lower in energy. The linear triplet OUCCO and bent CUO $^-$  species are trapped in both matrices with typical matrix shifts in their infrared spectra, but CUO fundamentals are displaced 195 and 68 cm $^{-1}$  from neon to argon. In addition to large neon-to-argon shifts, the isotopic frequency ratios (and normal modes) of CUO in neon and the CUO(Ar) $_x$  complex are substantially different. Similar experiments in krypton matrices give small shifts for CUO and OUCCO in the same states trapped in solid argon. In contrast, laser-ablated Th atoms react with CO to form CThO, which is trapped in the same bent triplet state in solid neon, argon and krypton.

Investigations with 2% Kr and 3% Xe in argon and 3% Xe in krypton give small shifts for CUO(Ng) $_n$  in the same triplet state trapped in solid argon. The Kr and Xe doped experiments give additional weak absorptions that evolve on annealing for three higher CUO(Kr) $_n$  and CUO(Xe) $_n$  complexes described as CUOAr $_{4-n}$ (Kr) $_n$ , CUOAr $_{4-n}$ (Xe) $_n$ , and CUO(Kr) $_{4-n}$ (Xe) $_n$  complexes. Relativistic density functional theory calculations show that distinct CUO(Ng) $_n$  complexes are responsible for these trends in frequencies and estimate the CUO–Ng dissociation energies as 3.7, 4.9 and 7.3 kcal/mol for Ar, Kr, and Xe, respectively.

(51) Seidel, S.; Seppelt, K. *Science* **2000**, *290*, 117.

(52) Pyykkö, P. *J. Am. Chem. Soc.* **1995**, *117*, 2067.

(53) Schröder, D.; Schwarz, H.; Hrusak, J.; Pyykkö, P. *Inorg. Chem.* **1998**, *37*, 624.

(50) Freeman, D. E.; Yoshino, K.; Tanaka, Y. *J. Chem. Phys.* **1974**, *61*, 4880.

**Acknowledgment.** We acknowledge support for this research from the NSF (CHE 00-78836 to L.A.) and the Division of Chemical Sciences, Geosciences, and Biosciences of the U.S. Department of Energy's Office of Basic Energy Sciences (DE-FG02-01ER15135 to B.E.B.). We thank A. W. Ehlers for providing the diffuse basis sets of Xe. We are grateful to the Ohio Supercomputer Center for generous grants of computer time. This research was performed in part using the Molecular

Science Computing Facility (MSCF) in the William R. Wiley Environmental Molecular Sciences Laboratory, a national scientific user facility sponsored by the U.S. Department of Energy's Office of Biological and Environmental Research and located at the Pacific Northwest National Laboratory. Pacific Northwest is operated for the Department of Energy by Battelle.

JA027819S